

9. Publications and Posters

List of Publications

1. Rajesh Bahekar, **Nandini Panchal**, Shubhangi Soman, Jigar Desai, Dipam Patel, Anil Argade, Archana Gite, Sanjay Gite, Bhaumin Patel, Sachchidanand S, Harilal Patel, Abhijit Chatterjee, Jogeswar Mahapatra, Hoshang Patel, Debducta Bandyopadhyay. Discovery of Potent Diaminopyrimidine-carboxamide Derivatives as JAK3 Selective Inhibitors. *Bioorganic chemistry*. **2020**, 99, 103851.

List of Posters

1. Nandini Panchal, Anil Argade, Archana Gite, Sanjay Gite, Bhaumin Patel, Krishnarup Ghoshdastidar, Debducta Bandyopadhyay, Poonam Giri, Jogeswar Mahapatra, Abhijit Chatterjee, Mukul Jain, Shubhangi Soman, Rajesh Bahekar, Jigar Desai. Design and synthesis of pyrimidine class of JAK inhibitors for the treatment of Rheumatoid Arthritis. Poster presented in 8th RBF international Symposium, Advances in New Drug Discovery Technologies And Translational Research at Zydus Research Centre, Ahmedabad in Feb 2-4, **2017**.

2. Nandini Panchal, Rajesh Bahekar, Shubhangi Soman, Jigar Desai, Archana Gite, Dipam Patel, Sanjay Gite, Bhaumin Patel, Sachchidanand S, Harilal Patel, Abhijit Chatterjee, Jogeswar Mahapatra, Hoshang Patela, Debducta Bandyopadhyay, Anil Argade. Synthesis and biological evaluation of Pyrimidine class of JAK inhibitors for the treatment of Rhumatoid Arthritis. Poster presented in 9th RBF international Symposium, Advances in New Drug Discovery and Development at Zydus Corporate Park, Ahmedabad in Feb 6-8, **2020**.



Contents lists available at ScienceDirect

Bioorganic Chemistry

journal homepage: www.elsevier.com/locate/bioorg

Discovery of diaminopyrimidine-carboxamide derivatives as JAK3 inhibitors[☆]



Rajesh Bahekar^{a,*}, Nandini Panchal^{a,b}, Shubhangi Soman^b, Jigar Desai^a, Dipam Patel^a, Anil Argade^a, Archana Gite^a, Sanjay Gite^a, Bhaumin Patel^a, Jeevan Kumar^c, Sachchidanand S^c, Harilal Patel^d, Rajesh Sundar^d, Abhijit Chatterjee^d, Jogeswar Mahapatra^d, Hoshang Patel^e, Krishnarup Ghoshdastidar^e, Debdutta Bandyopadhyay^e, Ranjit C. Desai^a

^a Department of Medicinal Chemistry, Zydus Research Centre, Sarkhej-Bavla, N.H. 8A Moraiya, Ahmedabad 382210, India

^b Department of Chemistry, Faculty of Science, M.S. University of Baroda, Vadodara 390002, India

^c Department of Bioinformatics, Zydus Research Centre, Sarkhej-Bavla, N.H. 8A Moraiya, Ahmedabad 382210, India

^d Department of Pharmacology, Zydus Research Centre, Sarkhej-Bavla, N.H. 8A Moraiya, Ahmedabad 382210, India

^e Department of Cell Biology, Zydus Research Centre, Sarkhej-Bavla, N.H. 8A Moraiya, Ahmedabad 382210, India

ABSTRACT

Selective inhibition of janus kinase (JAK) has been identified as an important strategy for the treatment of autoimmune disorders. Optimization at the C2 and C4-positions of pyrimidine ring of Cerdulatinib led to the discovery of a potent and orally bioavailable 2,4-diaminopyrimidine-5-carboxamide based JAK3 selective inhibitor (11i). A cellular selectivity study further confirmed that 11i preferentially inhibits JAK3 over JAK1, in JAK/STAT signaling pathway. Compound 11i showed good anti-arthritis activity, which could be correlated with its improved oral bioavailability. In the repeat dose acute toxicity study, 11i showed no adverse changes related to gross pathology and clinical signs, indicating that the new class JAK3 selective inhibitor could be viable therapeutic option for the treatment of rheumatoid arthritis.

1. Introduction

Rheumatoid arthritis (RA) is a chronic inflammatory disease characterized by synovitis and joint destruction [1,2]. The multiple cytokines (tumor necrosis factor- α (TNF- α) and interleukin (IL)) triggers RA pathogenesis by inducing intracellular signal transduction, via JAK/STAT (Janus kinases and signal transducers and activators of transcription) signaling pathway [3-6]. The JAK family of enzymes (JAK1, JAK2, JAK3 and tyrosine kinase 2 (TYK2)) are cytoplasmic protein tyrosine kinases, associated with various cytokine-mediated signal transduction pathways [7-9]. Binding of the cytokines to their corresponding receptors induces JAK activation and subsequent phosphorylation [10]. The activated JAKs phosphorylate STAT proteins, which translocate to the nucleus and promote cytokine-responsive gene expression [11]. Due to unique role of JAKs in the immune system, inhibition of JAKs emerged out as one of the most validated and attractive therapeutic target for the treatment of autoimmune disorders such as RA and other inflammatory diseases [12].

JAK3 is expressed in lymphoid cells, drives pro-inflammatory signaling cascades, inducing cytokine expression in the synovial fibroblasts,

activated monocytes and macrophages [13]. JAK3 pairs with the JAK1 and it is involved in common gamma chain (γ c) cytokine (IL-2, IL-4, IL-7, IL-9, IL-15 and IL-21) signaling pathways, which play important role in the T-cell differentiation, proliferation and survival [14].

Clinically, JAK1 inhibition induces undesirable secondary pharmacodynamic effects such as cholesterol and liver enzyme elevation [15]. JAK2 mediates signaling via hematopoietic cytokines such as erythropoietin (EPO), thus dose-limiting tolerability and safety issues such as anemia are being associated with the JAK2 inhibition [16]. Selective JAK3 inhibition only deters common gamma (γ c) chain receptors signaling and spares JAK1 dependent immunoregulatory cytokines (IL-10, IL-27 and IL-35) [17]. Thus, JAK3 selective inhibitors are likely to offer a better efficacy to the safety ratio in the clinic for the treatment of chronic inflammatory disorders.

2. Result and discussion

2.1. Design of novel JAK inhibitor

Over the past decades, structurally diverse JAK inhibitors were

[☆] ZRC communication No: 596 (Part of Ph.D thesis work of Nandini Panchal). * Corresponding author.

E-mail address: rajeshbahekar@zyduscadila.com (R. Bahekar).

<https://doi.org/10.1016/j.bioorg.2020.103851>

Received 4 December 2019; Received in revised form 10 April 2020; Accepted 12 April 2020

Available online 18 April 2020

0045-2068/ © 2020 Elsevier Inc. All rights reserved.

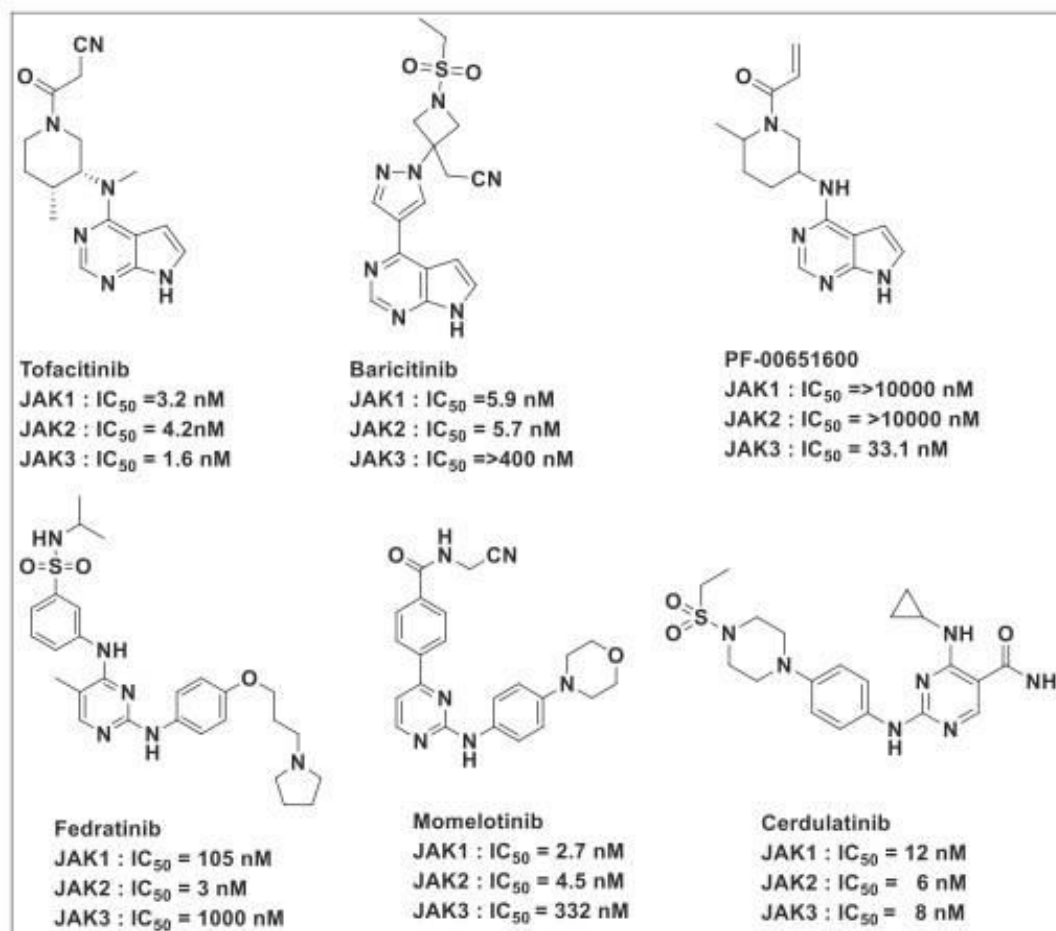


Fig. 1. Structures of 1H-pyrrolo[2,3-b]pyridine and Pyrimidine based JAK inhibitors.

identified containing pyrrolo [2,3-b]pyridine and pyrimidine core as a promising scaffold (Fig. 1) [18-20]. Tofacitinib, a low nanomolar (nM) JAK3 inhibitor but limited selectivity against JAK1 and JAK2 (Fig. 1) and the Baricitinib, a dual JAK1 and JAK2 inhibitor are approved for the treatment of RA [21,22]. Momelotinib, a dual JAK1 and JAK2 inhibitor and the Fedratinib, a JAK2 selective inhibitor are under clinical trials, for the treatment of myelofibrosis [23,24]. A reversible ATP-competitive dual SYK/JAK inhibitor, Cerdulatinib is under clinical trial for the treatment of leukemia and lymphoma [25]. Knowing the potential side effects associated with the PAN JAK inhibitors, efforts are being directed towards the development of a JAK3 selective inhibitor, for an effective treatment of autoimmune disorder [26].

Recently, JAK3 selective inhibitor programs have targeted covalent bond formation with Cys909 as an optimization strategy, including PF-06651600, an irreversible covalent inhibitor of JAK3 (Fig. 1), which is in the clinical trials for the treatment of inflammatory diseases [27-29]. Most of the irreversible JAK3 inhibitors demonstrated good JAK3 enzymatic selectivity but largely lacked cellular selectivity or appropriate physicochemical properties to be tested *in vivo* [30].

In this article, we present our efforts to develop novel non-covalent inhibitors of the JAK3. It was hypothesized that the non-covalent JAK3 selective inhibitors could be devoid of systemic toxicity. An approach undertaken to overcome the JAK isozymes selectivity was to capitalize on the amino acid sequence differences among the JAKs, more specifically to favor hydrogen bonding interaction with the JAK3 cysteine (Cys-909) residue in the catalytic domain to develop the novel, non-covalent JAK3 selective inhibitor. While designing JAK3 inhibitors, attempts were made to avoid an introduction of the covalent reactive

groups (CRGs), in the structural features to circumvent the possibility of a covalent modification of Cys-909.

Structural modifications were carried out in the Cerdulatinib (having pyrimidine moiety as a key pharmacophore, Fig. 1). In the docking studies (Fig. 3) Cerdulatinib showed hydrogen bonding interactions in the hinge region of JAK3 enzyme but no hydrogen bonding was observed in the catalytic domain. Initial attempts involved maintaining essential hydrogen bonding interactions in the original scaffold and optimization at the C2-position of pyrimidine ring of Cerdulatinib to induce additional hydrogen bonding with the Cys-909. Modifications at the C2 position of pyrimidine ring in the C4 benzylated Cerdulatinib (Set-1, Table 1) led to the single digit nM potent compound 5k, with moderate isoform selectivity (Table 3). Docking study of 5k reveals no additional hydrogen bonding in the catalytic domain of the JAK3.

In the second set (Table 2), changes were carried out at the C4-position of the 5k, mainly to improve JAK3 isoform selectivity, which led to the discovery of a novel 2,4-diaminopyrimidine-5-carboxamide based JAK3 selective inhibitor 11i. Docking study of 11i showed additional hydrogen bonding with the Cys-909 of JAK3 (Fig. 3) and no interaction with the Serine residue of JAK isoforms, in the ATP binding pockets. Based on the *in vitro* results, highly potent and selective compound (11i) was assessed *in vivo* for the pharmacokinetic (PK), efficacy and animal toxicity studies.

2.2. Chemistry

Synthesis of 2, 4-diaminopyrimidine-5-carboxamides derivatives (5a-o and 11a-o) was carried out as depicted in Scheme 1 and 2,

Table 1
Influence of modification at C2 position of Pyrimidine moiety on JAK3 inhibitory activity (*In vitro*).

Comp.	R ₁	JAK-3 IC ₅₀ (nM) ^a	Comp.	R ₁	JAK-3 IC ₅₀ (nM) ^a
5a		12.6	5i		48
5b		33.4	5j		102
5c		53.7	5k		9.5
5d		178	5l		22.4
5e		122	5m		56
5f		136	5n		66
5g		132	5o		89
5h		56	Cerdulatinib		8
			Tofacitinib		1.6

All the data are shown as the mean for at least two experiments.^aJAK3 inhibition (IC₅₀) determination using *in vitro* Fluorogenic substrate assays Kit from Millipore.

following the modified literature procedure [31]. Treatment of ethyl 4-chloro-2-(methylthio)pyrimidine-5-carboxylate (1) with benzyl amine gave 4-benzylamino carboxylate, followed by hydrolysis, to get the acid moiety (2). Compound 2 was converted into amide (3), using HOBt and EDC.HCl, followed by reaction with aq. ammonia. Compound 3 converted to reactive methyl sulfinyl derivative (4) using *m*-CPBA, followed by treatment with substituted aryl amines furnished compounds 5a-o. For the synthesis of 11a-o, substituted 4-hydroxy pyrimidine-5-carboxylate (6) was converted to reactive methyl sulfinyl derivative, using *m*-CPBA, followed by treatment with 4-aminophenylmethanesulfonate to get intermediate 7, which was converted to acid (8), using LiOH, as a base. Acid functionality of compound 8 transformed to amide (9), using aq. ammonia. Phenolic hydroxyl group of compound 9 was activated into reactive chloro group (10), using POCl₃, followed by reaction with substituted amines, furnished compounds 11a-o.

Compounds 5a-o and 11a-o were prepared in good yield (60 to 80%), under the mild reaction condition. Spectral data were found to be in conformity with the structures assigned, which ensure the formation of compounds 5a-o and 11a-o (see experimental section, 4.2).

2.3. JAK3 inhibitory activity (enzyme based biochemical screening)

For *in vitro* JAK3 inhibitory activity screening, Cerdulatinib and Tofacitinib were used as a positive control. In Set-1 (Table 1), 2-substituted diaminopyrimidine-5-carboxamides (5a-o) analogues displayed varying degree of JAK3 inhibitory activities. *m*-substituted *N*-phenyl derivatives, 5a (*m*-aniline), 5b (oxopropanamide), 5c (oxoacetic acid), 5d (cinnamamide), 5e (methanesulfonamide), 5f (sulfoximine) and 5g (sulfonylacetamide) showed moderate JAK3 inhibitory activity (IC₅₀: > 120 nM). Compounds 5h and 5i (positional isomer of 5e and 5f) exhibited enhanced JAK3 inhibitory activity (IC₅₀: 56 and 48 nM). Compound 5j (acetyl protection of 5h) displayed moderate JAK3 activity (IC₅₀: 102 nM). Replacement of the sulfonamide group (5h) with methane sulfonate (5k, IC₅₀: 9.5 nM) and isopropyl sulfonate (5l, IC₅₀: 22.4 nM) led to higher JAK3 inhibitory activity, whereas *o*-substitution with the electron donating groups such as amino (5m, IC₅₀: 56 nM), dimethylamine (5n, IC₅₀: 66 nM) and *N*-acetyl derivative (5o: IC₅₀: 89 nM) displayed comparatively weaker JAK3 inhibitory activity.

In Set-1, compound 5k (methane sulfonate) showed potent JAK3 inhibitory activity, which was found to be comparable to the

Table 2

Influence of modification at C4 position of Pyrimidine moiety on JAK3 inhibitory activity (*In vitro*).

Comp.	R ₂	JAK-3 IC ₅₀ (nM) ^a	Comp.	R ₂	JAK-3 IC ₅₀ (nM) ^a	
11a	H	300	11i		1.7	
11b		49	11j		256	
11c		37	11k		39	
11d		33	11l		43.2	
11e		79	11m		45.4	
11f		12	11n		49.2	
11g		9.8	11o		189	
11h		20	Cerdulatinib		8	
	Racemic		Tofacitinib		1.6	

All the data are shown as the mean for at least two experiments. ^aJAK3 inhibition (IC₅₀) determination using *in vitro* Fluorogenic substrate assays Kit from Millipore.

Cerdulatinib (IC₅₀: 8 nM; Table 1) and 5 fold less potent compared to Tofacitinib (IC₅₀: 1.6 nM). Thus, in the Set-1, substitution on *p*-position of phenyl ring, followed by replacement of *N*-acetyl to *O*-sulfonate led to the single digit nM potent compound (5k), with moderate isoform selectivity (Table 3).

Further, to improve JAK3 isoform selectivity, modifications were carried out in the 5k. In the second set (Table 2), variations were carried out at the C4-position of pyrimidine, in 5k. As listed in the Table 2 (compounds 11a-o), compound 11a (debenzylated 5k; IC₅₀: 300 nM) was found to be less active. Replacement of benzyl group with

Table 3

In vitro isoform selectivity of compounds against JAK1, JAK2 and TYK2 enzymes.

Compound	IC _{50a} (nM)				Selectivity fold		
	JAK1 ^b	JAK2 ^b	JAK3 ^b	TYK2 ^b	JAK1/ JAK3	JAK2/ JAK3	TYK2/ JAK3
5k	18	42	9.5	45	2	4	5
11i	20	171	1.7	186	12	100	109
Cerdulatinib	15	7	8	5	2	1	<1
Tofacitinib	3	5	1.6	34	2	3	21

^aThe IC₅₀ values are shown as the mean for at least two experiments. ^bJAK1, JAK2, JAK3, & TYK2 inhibitory assay Kit (Millipore) was used to screen the test compounds.

cycloalkyl groups, compound 11b (cyclopropyl, IC₅₀: 49 nM), 11c (cyclobutyl, IC₅₀: 37 nM), 11d (cyclopentyl, IC₅₀: 33 nM) and 11e (cyclohexyl, IC₅₀: 79 nM) showed moderate activities. Overall, the cycloalkyl derivatives were found to be less potent compared to 5k. Compound 11f (pyran, IC₅₀: 12 nM) showed slight improvement in the activity, while 11g (isobutane, IC₅₀: 9.8 nM) was found to be equipotent as the 5k. Racemic compound 11h (isopentane, IC₅₀: 20 nM) showed two fold less potency compared to 5k. Chirally pure compound 11i (R-isomer of 11h) was found to be five-fold more potent (IC₅₀: 1.7 nM), whereas 11j (S-isomer of 11h) was found to be least potent (IC₅₀: 256 nM). Compound 11k (phenyl ethyl, IC₅₀: 39 nM), fluoro-substituted benzyl analogues, 11l (3-fluoro), 11m (4-fluoro) and 11n (2-fluoro) showed moderate activities (IC₅₀ > 40 nM) compared to 5k, while 11o (naphthyl, IC₅₀: 189 nM) was found to be less active.

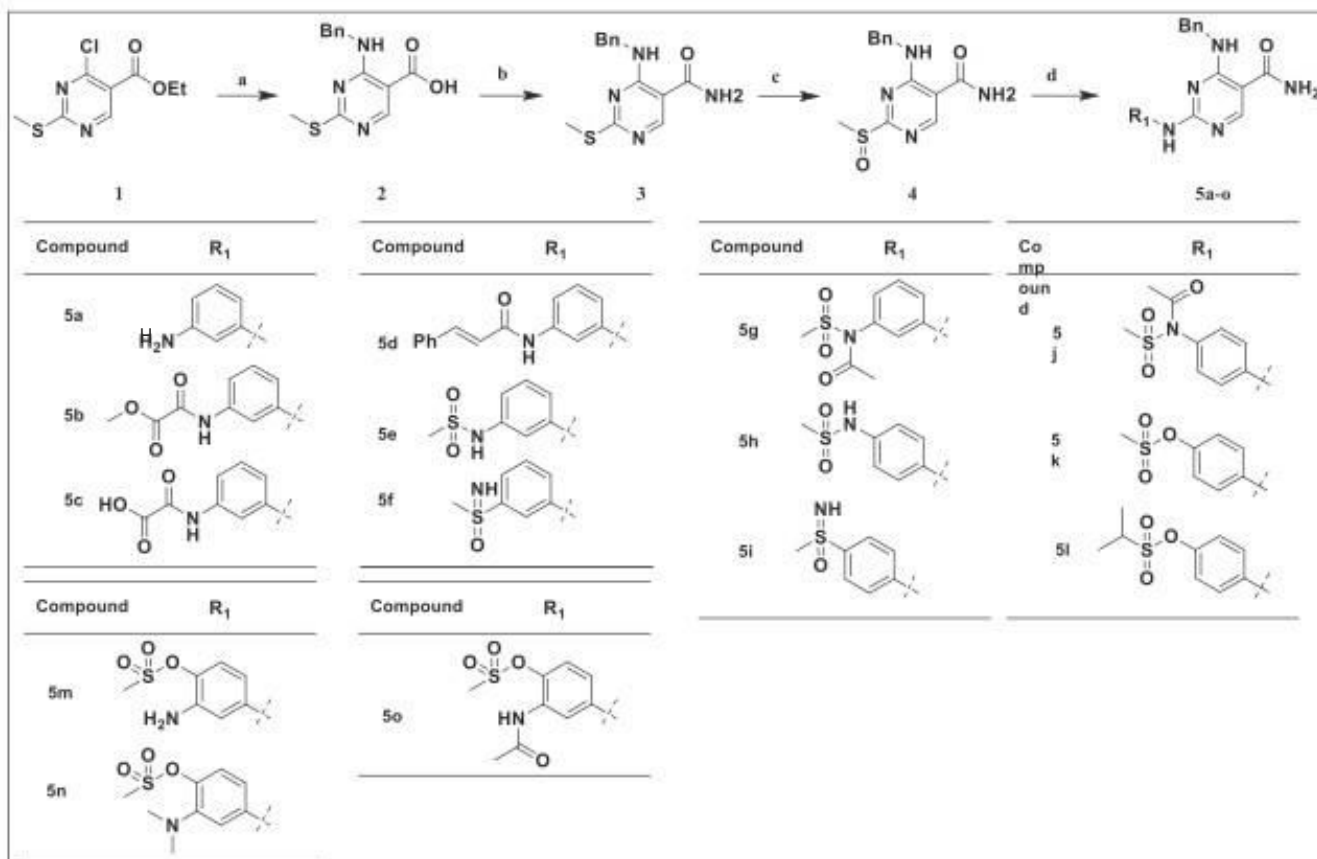
2.4. JAKs isoform selectivity (enzyme based biochemical screening)

Most potent compounds (5k and 11i) were evaluated for their selectivity against JAK isoforms (JAK-1, 2 and TYK2) [32]. As shown in Table 3, initial hit (5k) showed moderate selectivity (2 to 5X) against JAK isoforms over JAK3. Compound 11i (IC₅₀: 1.7 nM) demonstrated 12, 100, and 109 fold selectivity over JAK1, JAK2 and TYK2 respectively. Selectivity profile of 11i against all the three isoforms was found to be better than standard compounds. Thus, potency and selectivity of diaminopyrimidine-5-carboxamides based JAK3 inhibitors can be modulated using suitable substituents at C2 and C4-position of pyrimidine ring.

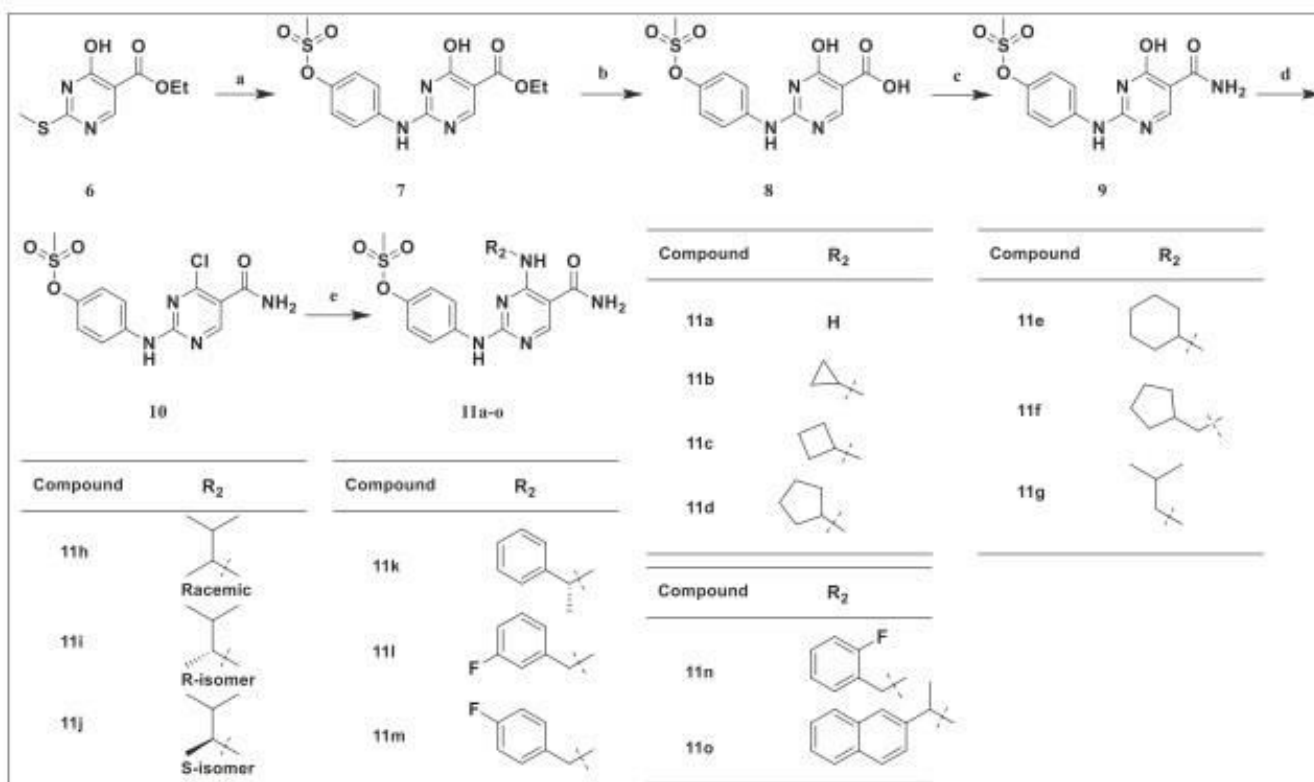
2.5. Profiling of 11i (*in vitro* and *ex vivo*)

In vitro kinase profiling study of compound 11i was carried out at 1 μM concentration, against Millipore panel of 170 purified kinases (n = 2) and the % inhibition was found to be < 20% at 1 μM concentration, including key cysteine containing protein kinases (TEC family (BMX, BTK, ITK, TXK, and TEC), ErbB family (EGFR, ERBB4, and ERBB2), CLK2, MKK7β, PKG1α and Aurora kinase), see Table 8.

JAK3 selectivity of 11i was evaluated under physiologic conditions (cellular assay) to understand role of the associated cytokine receptors and downstream inflammatory pathways inhibited. To elucidate potency and selectivity profile in a cellular environment, compound 11i was tested for the inhibition of phosphorylation of downstream signal (STAT proteins), in the human peripheral blood mononuclear cells (PBMCs) [33]. The different cellular stimuli were used to induce phosphorylation of STATs (pSTAT), either by dual JAK1/3 (IL-2 stimulus, pSTAT5), JAK2 (GM-CSF stimulus, pSTAT5), or with the PAN JAK1/JAK2/TYK2 (IL-6 stimulus, pSTAT3) stimuli [34]. As shown in Table 4, 11i showed 27-fold selectivity for inhibition of the IL-2 (IC₅₀: 22.16 nM) versus the IL-6 readout (IC₅₀: 608 nM) and a 23-fold selectivity for the inhibition of the GM-CSF (IC₅₀: 511 nM). Tofacitinib displayed similar potencies but lower selectivity than 11i in the



Scheme 1. Synthesis of Compound 5a-o. Reagents and conditions: a) Dioxane, DIPEA, Benzyl amine, 26 °C, 6 h, ii) Dioxane, LiOH, water, 26 °C, 6 h, 84% b) DMF, EDC.HCl, HOBT, Aq NH₃, 26 °C, 1 h, 95% c) Dioxane:CHCl₃ (1:1), m-CPBA, 50 mins, 10% sodium metabisulfate, 80% d) NMP,PTSA, R₁NH₂, 120 °C, 1 h.



Scheme 2. Synthesis of Compound 11a-o. Reagents and conditions: a) (i) Dioxane:CHCl₃(1:1), m-CPBA, 50 mins, 10% sodium metabisulfate, 80% (ii) NMP, PTSA, 4-aminophenylmethanesulfonate, 120 °C, 1 h, 75% b) THF, LiOH, water, 26 °C, 6 h, 80% c) DMF, EDC.HCl, HOBT, aq NH₃, 26 °C, 1 h, 70% d) Toluene, POCl₃, DIPEA, 120 °C, 3 h, 70% e) Dioxane, DIPEA, R₂NH₂, 26 °C, 6 h.

Table 4

Potency and selectivity determination of 11i in human PBMC.

JAKs involved	Trigger	Readout	IC ₅₀ (nM)		Selectivity	
			11i	Tofacitinib	11i	Tofacitinib
JAK1/3	IL-2	pSTAT5	22.16	25.22	-	-
JAK1/JAK2/TYK2	IL-6	pSTAT3	608	36.88	27.4	1.46
JAK2	GM-CSF	pSTAT5	511	210	23	8.32

IC₅₀ values in hPBMC were determined by plotting the compound concentration vs the effect on the readouts, using flow cytometry (n = 2).

relevant pSTAT assays. Thus, compound 11i showed preferential inhibition of JAK3 over JAK1, in the JAK/STAT signaling pathway, when assessed in the PBMC assay.

Ex vivo, compound 11i was evaluated for the plasma protein binding studies (using mice, rat and human plasma) and liver microsomal stability studies (using immortalized mice, rats and human liver cell line). Compound 11i showed 75 to 80% plasma protein binding and less than 10% metabolism at 30 min, in microsomal metabolic stability study. Compound 11i was found to be devoid of CYP (< 10% CYP inhibition) at

10 μM concentration, for CYP1A2, CYP2C8, CYP2C9, CYP2D6, CYP2C19 and CYP3A4 and hERG liabilities (IC₅₀: > 10 μM).

2.6. Pharmacokinetic study

In a single dose PK studies (3 mg/kg, po and 1 mg/kg, iv, in male C57BL/6J mice) of compounds 5k, 11i and Tofacitinib, various PK parameters (T_{max}, C_{max}, t_{1/2}, Cl, AUC and %F) were recorded (Table 5). Compound 5k showed moderate AUC, due to its high clearance, which resulted into overall low bioavailability (15%). Compound 11i showed higher AUC (~10 fold, compared to std), extended t_{1/2} (2.56 hr) and good oral bioavailability (%F: ~48 over std, 20%). Compound 11i showed extended t_{1/2} and higher AUC, which could be due to its low clearance compared to standard (11.59 vs 47.56 mL/min/kg, iv).

2.7. In vivo efficacy studies

2.7.1. Anti-arthritis efficacy of test compounds in collagen induced arthritis (CIA) mice model

Arthritis was developed in male DBA1j mice, using collagen mixture and mice were recruited for the study once clinical signs were visible [35]. Considering low bioavailability of 5k, only 11i was evaluated. Eight animals were assigned in each of the three groups [vehicle, positive control (Tofacitinib, 60 mg/kg) and test compound 11i (30 mg/kg)]. Treatment was continued for three weeks and percentage inhibition in clinical score was recorded.

As shown in the Fig. 2a, standard compound and 11i showed good reduction in the arthritic score, compared to vehicle control (untreated group). Two fold higher dose of a standard compound was used, considering > 2X difference in the mice oral bioavailability. At 30 mg/kg dose, compound 11i showed comparable anti-arthritis activity to that of standard compound (dose 60 mg/kg). Body weights of the animals

Table 5

Pharmacokinetic study parameters^a of 5k, 11i and Tofacitinib in C57 mice.

Compd	T _{max} (h)	C _{max} (ng/ml)	t _{1/2} (h)	Cl (ml/min/kg), iv	AUC (0-α) h μg/ml	%F*
5k	0.5	146 ± 48	1.85 ± 0.43	40.37 ± 3.61	192 ± 56	15
11i	0.25	1737.95 ± 205	2.56 ± 0.45	11.59 ± 1.65	2104 ± 487	48
Tofacitinib	0.25	80.39 ± 13.86	1.32 ± 0.65	47.56 ± 3.95	208.2 ± 35.7	20

^a In male C57BL/6J mice (n = 6), compounds were administered orally (po) at 3 mg/kg dose and plasma concentration was analyzed by LC-MS, values indicate Mean ± SD.

* Oral bioavailability (%F) was calculated wrt to iv AUC. Compounds 5k, 11i and Tofacitinib administered at 1 mg/kg dose, iv AUC (ng/ml): 412, 1459 and 350 respectively.

were also recorded 3 times a week as a measure of treatment related side effect. No changes in the mice body weight was observed in any treatment group, compared to vehicle control group. Thus improved PK of 11i justifies its potent *in vivo* efficacy in the CIA mice model.

2.7.2. Anti-arthritis efficacy of test compounds in AIA (Adjuvant induced Arthritis) rat model

Anti-arthritis efficacy of the compound 11i was evaluated in a rat AIA model [36]. As shown in the Fig. 2b, standard and 11i showed good reduction in the paw volume, compared to vehicle control (untreated group). Compound 11i suppressed paw swelling in a dose-dependent manner (ED₅₀: 10 mg/kg) and at 30 mg/kg dose, efficacy of 11i was found to be comparable to that of standard (Tofacitinib, 60 mg/kg). Body weight was not significantly affected in rats, in any treatment group compared to the vehicle control group.

2.8. Safety pharmacology

To assess the safety profile of compound 11i, repeat dose acute toxicity studies (14 days) was carried out in male Wistar rats (100 mg/kg, po, once daily) and various parameters such as gross pathology, clinical signs, body weight, organ weight and serum chemistry/hematological changes were recorded. Daily oral administration of compounds 11i (10X of ED₅₀ dose), over a period of 2 weeks did not affect the survival of Wistar rats and also no adverse changes related to gross pathology, clinical signs, body weight and feed consumption were noticed, compared to control group. As shown in Tables 6 and 7, the hematological parameters (WBC and RBC) of compounds 11i were found to be comparable to that of control animals. Similarly, compound 11i showed no significant changes in serum hepatotoxicity assessment parameters as compared to the control group. Also compound 11i treated groups showed no changes in the key organs (heart, kidney, spleen and brain) weights.

2.9. Docking study

In the docking studies, Cerdulatinib binds in a similar orientation to that of 4,6-diaminonicotinamide of the co-crystallized ligand (9YV; 4-(benzylamino)-6-({4-[(1-methylpiperidin-4-yl)carbamoyl]phenyl}amino)pyridine-3-carboxamide), maintaining hydrogen bonding interactions with the hinge region of JAK3 (a 'classical' triad hinge binding interaction), Fig. 3. The docked poses of the core of Cerdulatinib and the co-crystallized ligand superimposed well. Compound 11i showed similar interactions as that of Cerdulatinib, in the hinge region and superimposed very well with the core of Cerdulatinib. However, 11i showed additional interaction with the Cys909 (hydrogen bond between NH of Cys909 with oxygen of methyl sulfonate group), which was not observed with the Cerdulatinib. An additional interactions of 11i with the Cys909, in the catalytic domain of JAK3 enzyme likely to contribute towards its potent and selective JAK3 inhibitory activity. The docking score for Cerdulatinib and 11i was found to be -8.6 and -9.9 kcal mol⁻¹ respectively.

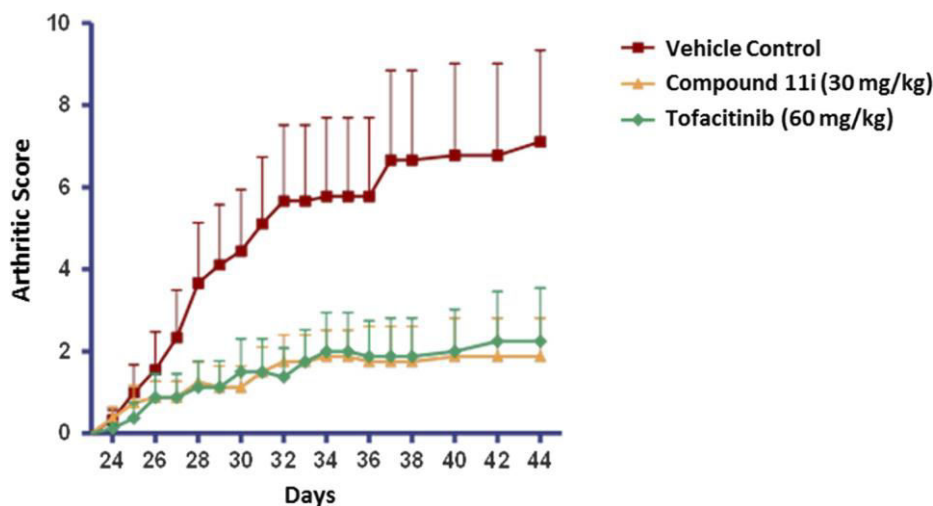


Fig. 2a. Effect of Compound 11i and Tofacitinib in CIA mice model.

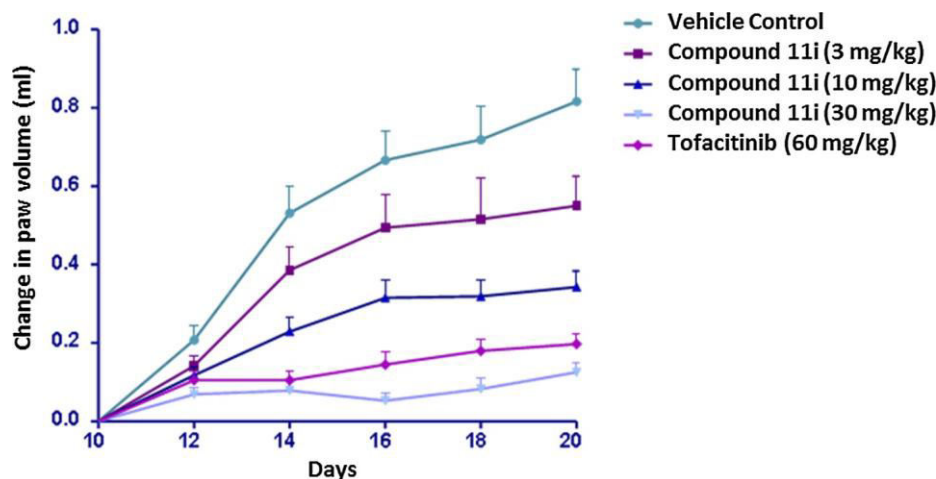


Fig. 2b. Effect of Compound 11i and Tofacitinib in AIA rat model.

3. Conclusion

In summary, we have described discovery and characterization of a novel JAK3 inhibitor, compound 11i. Two series of 2,4-diaminopyrimidine-5-carboxamide derivatives were evaluated as a JAK3 inhibitors. Modifications at the C2-position of pyrimidine ring led to an identification of a single digit nM potent JAK3 inhibitor (5k), with moderate isoform selectivity. Further structure-activity relationship (SAR) studies on the C4-position of 5k resulted in to the discovery of (R)-4-((5-carbamoyl-4-((3-methylbutan-2-yl)amino)pyrimidin-2-yl)amino)phenyl methane sulfonate (11i) that showed improved isoform selectivity in the biochemical assay. Compound 11i selectively inhibits JAK3 cytokine signaling in the primary cells, which translated to the promising efficacy in animal models of RA. In the repeat dose acute toxicity study, 11i showed no adverse changes related to gross pathology, clinical signs and liver toxicity, indicating that the new class JAK3 selective inhibitor could be viable therapeutic option for the treatment of rheumatoid arthritis.

4. Experimental section

4.1. Materials and methods

NMR spectra were measured on a Varian Unity 400 (^1H at 400 MHz, ^{13}C at 100 MHz), magnetic resonance spectrometer. Spectra were taken

in the indicated solvent at ambient temperature. Chemical shifts (δ) are given in parts per million (ppm) with tetramethylsilane as an internal standard. Multiplicities are recorded as follows: s = singlet, d = doublet, t = triplet, q = quartet, br = broad, m = multiplet. Coupling constants (J values) are given in Hz. Mass spectra are recorded on Perkin-Elmer Sciex API 3000. Reactions were monitored using thin layer silica gel chromatography (TLC) using 0.25 mm silica gel 60F plates from Merck. Plates were visualized by treatment with UV, acidic p-anisaldehyde stain, KMnO_4 stain with gentle heating. Products were purified by column chromatography using silica gel 100-200 mesh and the solvent systems indicated.

4.2. General synthesis

4.2.1. 4-(Benzylamino)-2-(methylthio)pyrimidine-5-carboxylic acid (2)

Ethyl 4-chloro-2-(methylthio)pyrimidine 5-carboxylate (1) 13.3 g (57.2 mmol) dissolved in dioxane 100 mL and DIPEA 10.99 mL (62.9 mmol) was added to the reaction mixture at 0 °C, followed by addition of benzyl amine 6.13 g (57.2 mmol) and the reaction mixture was stirred at 0 °C for 30 min, and then 6 h. at RT. LiOH 6.85 g (286 mmol) was dissolved in 50 mL water and added in to reaction mixture and stirred overnight at 28 °C. After completion of reaction, the reaction mixture was concentrated by rotary evaporation to remove a majority of the dioxane, and then acidified with 10 M HCl to pH ~ 5, resulting in the formation of a white precipitate. The solid compound

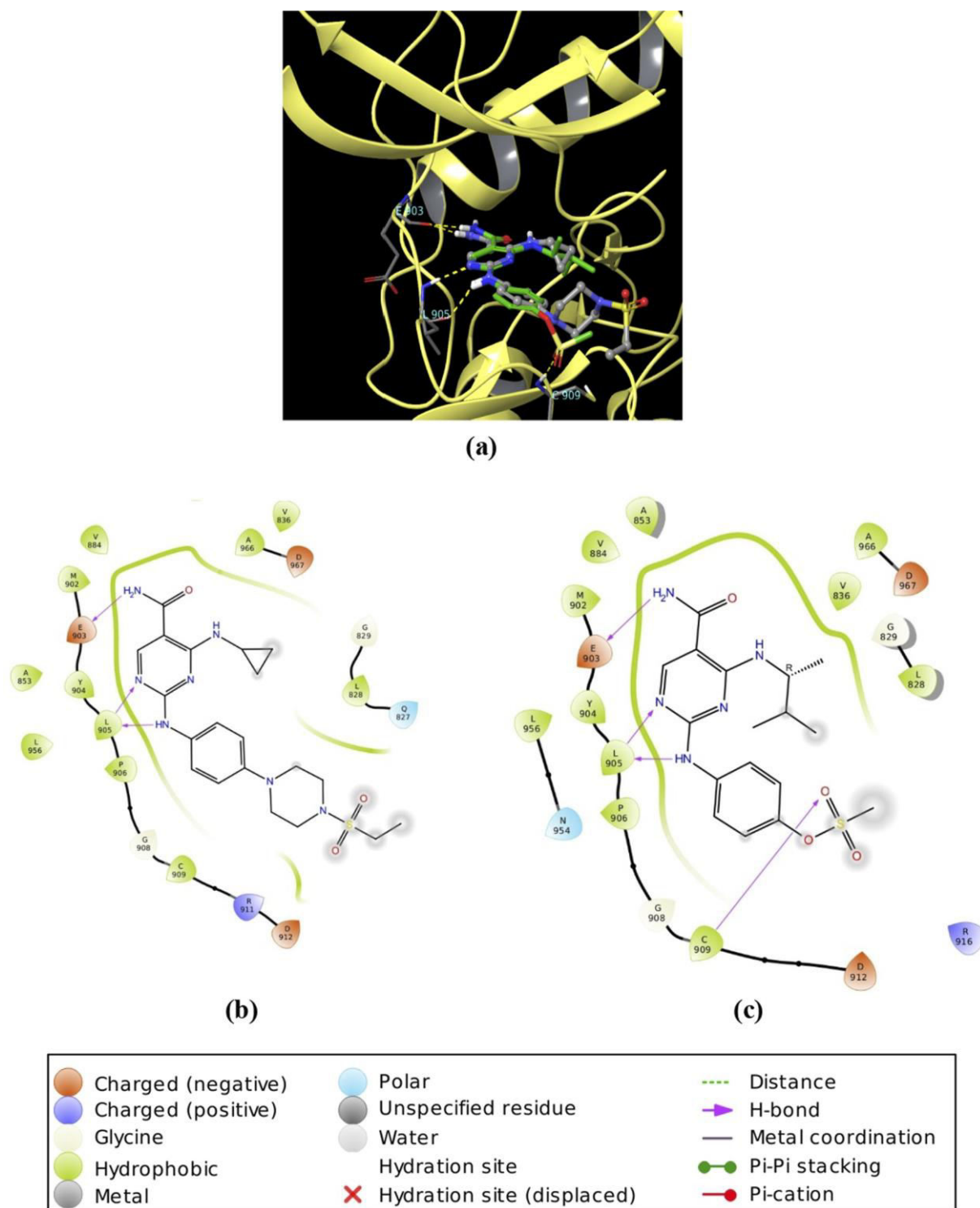


Fig. 3. Docked pose of Cerdulatinib and 11i within ATP binding site of JAK3 molecular surface (PDB ID: 5 W86 @2.6 Å). (a) Docked pose of Cerdulatinib and 11i superimposed (Cerdulatinib is shown in ball and stick model with grey carbon while 11i is displayed in stick model with green carbon), yellow dashed lines shows the H-bond interactions. (b) 2D Ligand interaction diagram of Cerdulatinib and (c) 2D Ligand interaction diagram of 11i (carbon is shown in grey), with residues within 4 Å, hydrogen bonds are shown with arrows.

was filtered, washed with water and dried under vacuum to afford the 4-(benzylamino)-2-(methylthio)pyrimidine-5-carboxylic acid (2) as white solid. (13.23 g, 84%). $^1\text{H NMR}$ ($\text{DMSO}-d_6$, 400 MHz) δ ppm: 2.59 (s, 3H), 4.69 (d, $J = 6.0$ Hz, 3H), 7.28-7.22 (m, 1H), 7.30-7.33 (m, 4H), 8.52 (s, 1H), 9.25 (s, 1H). ESI-MS: m/z Calcd for $\text{C}_{13}\text{H}_{14}\text{N}_3\text{O}_2\text{S}$ [$\text{M} + 1$] $^+$ 276.33, found 276.05.

4.2.2. 4-(Benzylamino)-2-(methylthio)pyrimidine-5-carboxamide (3)

4-(Benzylamino)-2-(methylthio)pyrimidine-5-carboxylic acid (2) 12 g (43.6 mmol) was dissolved in DMF 100 mL, under nitrogen atmosphere and treated with HOBT 6.68 g (43.6 mmol) and EDC.HCl 16.68 g (87.0 mmol) at RT. After stirring 1 hr., aq. Ammonia (40 mL) was added at 0° C, and it was stirred further for 1 h., at RT. Reaction mixture was quenched by ice - water (200 mL), resulted in the

Table 6
Hematological parameters and serum chemistry of compound 11i.^a

Parameters	Compound	
	Control 11i ^a	
RBC (10 ⁶ μl ⁻¹)	7.25 ± 0.19	8.35 ± 0.33
AST (U L ⁻¹)	146.88 ± 11.54	139.71 ± 9.50
TBILI (mg dL ⁻¹)	0.15.50 ± 0.05	0.18 ± 0.12
WBC (10 ³ μl ⁻¹)	9.10 ± 0.35	8.99 ± 0.30
ALT (U L ⁻¹)	19.97 ± 1.55	20.69 ± 8.63
ALP (U L ⁻¹)	135.21 ± 5.78	120.80 ± 12.9

^a Values expressed as mean ± SD; n = 9, Male WR dose 100 mg kg⁻¹, po (bid), 14 days repeated dose toxicity study.

Table 7
Relative organ weights (%) after 14 days repeat dose treatment with compound 11i.^a

Organs	Compounds	
	Control (Vehicle) 11i ^a (100 mg kg ⁻¹ , po, bid)	
Brain	0.730 ± 0.028	0.690 ± 0.03
Kidney	0.800 ± 0.034	0.814 ± 0.03
Heart	0.350 ± 0.009	0.360 ± 0.007
Spleen	0.250 ± 0.006	0.243 ± 0.01
Liver	3.598 ± 0.15	3.660 ± 0.078

^a Values expressed as mean ± SD; n = 9, Male WR, dose 100 mg kg⁻¹, po (bid), 14 days repeated dose toxicity study.

formation of a white precipitate. The solid compound was filtered, washed with water and dried under to afford 4-(benzylamino)-2-(methylthio)pyrimidine-5-carboxamide (3) (11.36 g, 95%). ¹H NMR (DMSO-*d*₆, 400 MHz) δ ppm: 2.40 (s, 3H), 4.67 (d, *J* = 6.0 Hz, 2H), 7.23-7.28 (m, 1H), 7.31-7.35 (m, 4H), 7.45 (s, 1H), 8.04 (s, 1H), 8.53 (s, 1H), 9.48 (t, *J* = 6.0 Hz, 1H). ESI-MS: *m/z* Calcd for C₁₃H₁₅N₄OS [M + 1]⁺ 275.34, found 275.08.

4.2.3. 4-(Benzylamino)-2-(methylsulfinyl)pyrimidine-5-carboxamide (4)

4-(Benzylamino)-2-(methylthio)pyrimidine-5-carboxamide (3; 11 g (40.1 mmol)) was dissolved in a mixture of dioxane and chloroform (1:1; 290 mL). Reaction mixture was cooled up to -2°C and treated with *m*-CPBA (60%; 17.3 g, 60.1 mmol) and it was stirred for 50 min at 0 °C. Reaction mixture was quenched with 10% aq. sodium metabisulfite (290 mL) and extracted with chloroform. Organic layer was washed with aq. 10% sodium bicarbonate. The organic layer was dried over sodium sulfate (42 g) and the solvent was removed under reduced pressure to afford 4-(benzylamino)-2-(methylsulfinyl)pyrimidine-5-carboxamide (4) as white solid. (9.31 g, 80%). ¹H NMR (DMSO-*d*₆, 400 MHz) δ ppm 2.75 (s, 3H), 4.70 (d, *J* = 6.0 Hz, 2H), 7.24-7.31 (m, 1H), 7.33-7.38 (s, 4H), 7.74 (s, 1H), 8.28 (s, 1H), 8.76 (s, 1H), 9.60 (t, *J* = 5.6 Hz, 2H). ESI-MS: *m/z* Calcd for C₁₃H₁₅N₄O₂S [M + 1]⁺ 291.34, found 291.00.

4.2.4. General procedure for the synthesis of compound 5a-o

To a solution of 4-(benzylamino)-2-(methylsulfinyl)pyrimidine-5-carboxamide (4; 1.0 eq) and PTSA (1.1 eq), in NMP was added different substituted aryl amines (1.0 eq), at RT. The reaction mixture was heated at 100-110 °C for 1-2 h. After completion of reaction, the mixture was diluted with water and the compound was extracted in EtOAc. Organic layer was dried over sodium sulfate, filtered and concentrated under vacuum to afford the crude product. Crude product was purified by flash chromatography over silica gel (100-200 mesh) with 2% MeOH/CHCl₃ to provide the desired title product 5a-o.

4.2.4.1. 2-((3-Aminophenyl)amino)-4-(benzylamino)pyrimidine-5-carboxamide (5a). Refer to general procedure for the synthesis of 5a, as

Table 8
Kinome Selectivity Profile of 11i.^a

Kinase	%	Kinase	%	Kinase	%
ACK1	12	B-Raf	07	CDK2	10
PKA	13	MAPK1	13	CDK6	02
IR	03	PRK2	20	CDK7	03
Lck	19	IGF-1R	10	CDK9	09
Mer	11	JNK1α1	10	Plk3	03
KDR	00	JNK2α2	05	TAO1	13
SGK	05	PAK4	14	Aurora-A	15
DDR1	18	GCK	19	Aurora-B	19
Syk	00	Pim-1	16	MST1	19
Rsk2	20	Pim-2	05	TBK1	02
ZIPK	00	SAPK2a	01	TrkA	12
Src	09	SAPK2b	07	TrkB	18
ROCK-I	16	SAPK3	09	TrkC	16
ROCK-II	13	SAPK4	02	NEK2	02
FAK	19	MAPKAP-K2	02	Fms	04
STK33	09	Wee1	12	CaMK1	02
JAK3	99.2	MSK1	17	CaMKIIβ	18
Ret	12	Fyn	05	CaMKK2	06
ALK	02	Ab1	03	Lyn	08
ALK4	01	CDK1	09	MEK1	10
Flt1	02	FGFR1	12	PKG1α	19
Flt3	16	DYRK1A	05	GRK5	08
PDGFRα	03	DYRK1B	12	GSK3α	16
CK1	20	CLK2	15	GSK3β	07
MKK4	06	IKKα	02	PKBα	04
MKK6	19	IKKβ	09	PKCθ	17
MKK7β	17	IKKε	01	PKCξ	10

^a Values represent percent inhibition at 1 μM concentration, listed key 91 kinase as representative data as mean of 2 independent measurements. Higher numbers indicate stronger binding, DMSO used as negative control (% inhibition = 0%).

described in section 4.1.4. 51.2% isolated yield; white solid. ¹H NMR (DMSO-*d*₆, 400 MHz) δ ppm 4.67 (d, *J* = 5.6 Hz, 2H), 6.18 (d, *J* = 6.8 Hz, 1H), 6.82-6.86 (m, 2H), 6.97 (s, 1H), 7.22-7.35 (m, 5H), 8.51 (s, 1H), 9.20 (s, 1H), 9.47 (t, *J* = 6 Hz, 1H). ¹³C NMR (DMSO-*d*₆, 100 MHz) δ ppm 43.9, 100.5, 100.9, 103.2, 107.0, 126.6, 127.0, 128.7, 129.5, 139.9, 142.9, 148.0, 161.8, 165.1, 166.2, 169.6. ESI-MS: *m/z* Calcd for C₁₈H₁₉N₆O [M + 1]⁺ 335.38, found 334.90.

4.2.4.2. Methyl-2-((3-((4-(Benzylamino)-5-carbamoylpyrimidin-2-yl)amino)phenyl)amino)-2-oxoacetate (5b). Refer to general procedure for the synthesis of 5b, as described in section 4.1.4. 49.5% isolated yield; white solid. ¹H NMR (DMSO-*d*₆, 400 MHz) δ ppm 3.84 (s, 3H), 4.72 (d, *J* = 6.0 Hz, 2H), 7.18-7.31 (m, 8H), 8.25 (s, 1H), 8.55 (s, 1H), 9.71 (s, 2H), 10.68 (s, 1H). ¹³C NMR (DMSO-*d*₆, 100 MHz) δ ppm 43.8, 51.1, 100.4, 107.8, 111.0, 113.6, 126.5, 127.1, 128.8, 129.6, 137.2, 140.0, 142.7, 155.0, 162.2, 164.5, 165.9, 166.8, 169.7. ESI-MS: *m/z* Calcd for C₂₁H₂₁N₆O₄ [M]⁺ 420.43, found 420.80.

4.2.4.3. 2-((3-((4-(Benzylamino)-5-carbamoylpyrimidin-2-yl)amino)phenyl)amino)-2-oxoacetic acid (5c). Refer to general procedure for the synthesis of 5c, as described in section 4.1.4. 51.9% isolated yield; white solid. ¹H NMR (DMSO-*d*₆, 400 MHz) δ ppm 4.71 (d, *J* = 6.0 Hz, 2H), 6.98-7.70 (m, 7H), 7.86-7.94 (m, 1H), 8.17 (s, 1H), 8.53 (s, 1H), 9.62 (s, 2H), 10.58 (s, 1H). ¹³C NMR (DMSO-*d*₆, 100 MHz) δ ppm 43.8, 100.5, 107.9, 110.9, 113.8, 126.5, 127.1, 128.8, 129.9, 137.8, 140.1, 143.0, 156.9, 162.0, 164.1, 166.0, 166.9, 169.5. ESI-MS: *m/z* Calcd for C₂₀H₁₈N₆O₄ [M]⁺ 406.40, found 406.02.

4.2.4.4. 4-(Benzylamino)-2-((3-cinnamidophenyl)amino)pyrimidine-5-carboxamide (5d). Refer to general procedure for the synthesis of 5d, as described in section 4.1.4. 48.8% isolated yield; white solid. ¹H NMR (DMSO-*d*₆, 400 MHz) δ ppm 4.74 (d, *J* = 6.0 Hz, 2H), 6.84 (s, 1H), 6.88 (s, 1H), 7.21-7.32 (m, 5H), 7.38-7.45 (m, 5H), 7.47-7.61 (m, 3H), 8.14 (s, 1H), 8.56 (s, 1H), 9.53 (s, 2H), 10.11 (s, 1H). ¹³C NMR (DMSO-*d*₆,

100 MHz) δ ppm 43.5, 100.4, 108.0, 111.2, 113.9, 119.0, 126.7, 127.4, 128.0, 128.4, 128.7, 128.9, 129.6, 135.6, 137.1, 139.8, 142.0, 143.2, 162.2, 165.8, 166.7, 167.2, 169.8. ESI-MS: m/z Calcd for $C_{27}H_{25}N_6O_2$ $[M]^+$ 464.53, found 464.90.

4.2.4.5. 4-(benzylamino)-2-((3-(methylsulfonamido)phenyl)amino)pyrimidine-5-carboxamide (5e). Refer to general procedure for the synthesis of 5e, as described in section 4.1.4. 50.8% isolated yield; white solid. 1H NMR (DMSO- d_6 , 400 MHz) δ ppm 3.33 (s, 3H), 4.70 (d, $J = 5.6$ Hz, 2H), 7.10-7.05 (m, 2H), 7.31-7.35 (m, 4H), 7.80-7.88 (m, 2H), 7.94 (s, 1H), 8.59 (s, 1H), 9.55 (s, 1H), 9.69 (s, 1H). ^{13}C NMR (DMSO- d_6 , 100 MHz) δ ppm 40.0, 44.5, 101.0, 101.5, 107.4, 109.0, 126.5, 127.1, 128.6, 130.0, 138.3, 139.5, 143.0, 161.9, 165.5, 167.0, 169.1. ESI-MS: m/z Calcd for $C_{19}H_{20}N_6O_3S$ $[M]^+$ 412.47, found 412.22.

4.2.4.6. 4-(Benzylamino)-2-((3-(S-methylsulfonimidoyl)phenyl)amino)pyrimidine-5-carboxamide (5f). Refer to general procedure for the synthesis of 5f, as described in section 4.1.4. 45.9% isolated yield; white solid. 1H NMR (DMSO- d_6 , 400 MHz) δ ppm 2.51 (s, 3H), 4.65 (d, $J = 6.0$ Hz, 2H), 6.80-6.87 (m, 2H), 7.26-7.27 (m, 5H), 7.33-7.34 (m, 2H), 8.37 (s, 1H), 9.61 (s, 1H), 9.78 (s, 1H). ^{13}C NMR (DMSO- d_6 , 100 MHz) δ ppm 43.8, 44.2, 100.9, 112.2, 114.5, 120.3, 126.8, 127.0, 128.7, 128.9, 140.1, 142.3, 146.8, 162.0, 165.9, 168.2, 169.8. ESI-MS: m/z Calcd for $C_{19}H_{20}N_6O_2S$ $[M]^+$ 396.47, found 396.20.

4.2.4.7. 4-(Benzylamino)-2-((3-(N-(methylsulfonyl)acetamido)phenyl)amino)pyrimidine-5-carboxamide (5g). Refer to general procedure for the synthesis of 5g, as described in section 4.1.4. 49.6% isolated yield; white solid. 1H NMR (DMSO- d_6 , 400 MHz) δ ppm 1.83 (s, 3H), 3.46 (s, 3H), 4.70 (d, $J = 6.0$ Hz, 2H), 7.03 (d, $J = 7.2$ Hz, 1H), 7.23-7.26 (m, 1H), 7.31-7.35 (m, 5H), 7.66 (d, $J = 7.2$ Hz, 1H), 7.93 (s, 1H), 8.59 (s, 1H), 9.64 (s, 1H), 9.75 (s, 1H). ^{13}C NMR (DMSO- d_6 , 100 MHz) δ ppm 20.0, 43.7, 44.0, 101.2, 108.4, 113.9, 119.9, 126.9, 127.2, 128.6, 129.1, 131.5, 140.0, 142.5, 162.3, 166.2, 166.5, 168.5, 169.7. ESI-MS: m/z Calcd for $C_{21}H_{23}N_6O_4S$ $[M+1]^+$ 455.50, found 455.00.

4.2.4.8. 4-(Benzylamino)-2-((4-(methylsulfonamido)phenyl)amino)pyrimidine-5-carboxamide (5h). Refer to general procedure for the synthesis of 5h, as described in section 4.1.4. 47.8% isolated yield; white solid. 1H NMR (DMSO- d_6 , 400 MHz) δ ppm 2.90 (s, 3H), 4.67 (d, $J = 6.0$ Hz, 2H), 7.05 (d, $J = 9.2$ Hz, 2H), 7.32-7.33 (m, 5H), 7.58 (d, $J = 8.8$ Hz, 2H), 8.54 (s, 1H), 9.39 (s, 1H), 9.45 (s, 1H), 9.47 (s, 1H). ^{13}C NMR (DMSO- d_6 , 100 MHz) δ ppm 43.9, 43.6, 100.8, 117.9, 118.6, 126.6, 126.9, 127.8, 128.2, 128.9, 139.8, 162.5, 166.2, 168.5, 169.8. ESI-MS: m/z Calcd for $C_{19}H_{20}N_6O_3S$ $[M]^+$ 412.47, found 412.80.

4.2.4.9. 4-(Benzylamino)-2-((4-(S-methylsulfonimidoyl)phenyl)amino)pyrimidine-5-carboxamide (5i). Refer to general procedure for the synthesis of 5i, as described in section 4.1.4. 45.2% isolated yield; white solid. 1H NMR (DMSO- d_6 , 400 MHz) δ ppm 2.50 (s, 3H), 4.41 (d, $J = 6.0$ Hz, 2H), 6.64 (d, $J = 8.8$ Hz, 2H), 7.22-7.32 (m, 5H), 7.54 (d, $J = 8.0$ Hz, 2H), 8.45 (s, 1H), 9.42 (s, 1H), 9.65 (s, 1H). ^{13}C NMR (DMSO- d_6 , 100 MHz) δ ppm 43.8, 45.2, 101.7, 115.0, 126.2, 126.5, 126.7, 128.0, 136.2, 140.0, 141.3, 162.4, 166.1, 168.8, 169.5. ESI-MS: m/z Calcd for $C_{19}H_{20}N_6O_2S$ $[M]^+$ 396.47, found 396.80.

4.2.4.10. 4-(Benzylamino)-2-((4-(N-(methylsulfonyl)acetamido)phenyl)amino)pyrimidine-5-carboxamide (5j). Refer to general procedure for the synthesis of 5j, as described in section 4.1.4. 49.7% isolated yield; white solid. 1H NMR (DMSO- d_6 , 400 MHz) δ ppm 1.88 (s, 3H), 3.49 (s, 3H), 4.70 (d, $J = 6.0$ Hz, 2H), 7.22-7.31 (m, 5H), 7.33-7.36 (m, 2H), 7.78 (d, $J = 8.8$ Hz, 2H), 8.58 (s, 1H), 9.57 (t, $J = 6.0$ Hz, 1H), 9.74 (s, 1H). ^{13}C NMR (DMSO- d_6 , 100 MHz) δ ppm 19.5, 42.9, 43.7, 100.5, 117.6, 119.6, 121.8, 126.4, 126.9, 127.9, 139.7, 140.1, 162.8, 166.9, 167.2, 168.8, 169.2. ESI-MS m/z Calcd for $C_{21}H_{23}N_6O_4S$ $[M]^+$ 454.50, found 454.90.

4.2.4.11. 4-((4-(Benzylamino)-5-carbamoylpyrimidin-2-yl)amino)phenyl methanesulfonate (5k). Refer to general procedure for the synthesis of 5k, as described in section 4.1.4. 51.5% isolated yield; white solid. 1H NMR (DMSO- d_6 , 400 MHz) δ ppm 3.33 (s, 3H), 4.68 (d, $J = 5.6$ Hz, 2H), 7.18 (d, $J = 8.4$ Hz, 2H), 7.22-7.35 (m, 5H), 7.73 (d, $J = 8.4$ Hz, 2H), 8.56 (s, 1H), 9.57 (s, 1H), 9.66 (s, 1H). ^{13}C NMR (DMSO- d_6 , 100 MHz) δ ppm 37.5, 44.0, 100.5, 120.5, 122.6, 127.4, 127.8, 128.9, 139.8, 143.5, 157.7, 160.2, 161.9, 169.4. ESI-MS: m/z Calcd for $C_{19}H_{20}N_6O_4S$ $[M]^+$ 413.45, found 413.90.

4.2.4.12. 4-((4-(Benzylamino)-5-carbamoylpyrimidin-2-yl)amino)phenyl propane-2-sulfonate (5l). Refer to general procedure for the synthesis of 5l, as described in section 4.1.4. 50.5% isolated yield; white solid. 1H NMR (DMSO- d_6 , 400 MHz) δ ppm 1.41 (d, $J = 6.8$ Hz, 6H), 3.64-3.67 (m, 1H), 4.68 (d, $J = 6.0$ Hz, 2H), 7.13 (d, $J = 9.2$ Hz, 2H), 7.23-7.34 (m, 5H), 7.71 (d, $J = 9.2$ Hz, 2H), 8.56 (s, 1H), 9.55 (s, 1H), 9.65 (s, 1H). ^{13}C NMR (DMSO- d_6 , 100 MHz) δ ppm 16.0, 43.8, 49.8, 100.7, 121.0, 122.4, 127.3, 127.7, 128.6, 138.9, 142.9, 158.0, 160.9, 162.2, 169.8. ESI-MS: m/z Calcd for $C_{21}H_{24}N_6O_4S$ $[M+1]^+$ 442.51, found 442.10.

4.2.4.13. 2-Amino-4-((4-(benzylamino)-5-carbamoylpyrimidin-2-yl)amino)phenyl methane sulfonate (5m). Refer to general procedure for the synthesis of 5m, as described in section 4.1.4. 49.8% isolated yield; white solid. 1H NMR (DMSO- d_6 , 400 MHz) δ ppm 3.33 (s, 3H), 4.68 (d, $J = 6.0$ Hz, 2H), 5.18 (s, 2H), 6.88-6.95 (m, 2H), 7.19-7.26 (m, 2H), 7.30-7.36 (m, 4H), 8.53 (s, 1H), 9.37 (s, 1H), 9.49 (t, $J = 5.8$ Hz, 2H). ^{13}C NMR (DMSO- d_6 , 100 MHz) δ ppm 37.9, 44.0, 100.1, 107.1, 108.1, 123.2, 127.3, 127.7, 128.8, 130.7, 139.9, 140.0, 141.1, 157.7, 160.4, 161.9, 169.5. ESI-MS: m/z Calcd for $C_{19}H_{21}N_6O_4S$ $[M+1]^+$ 429.47, found 429.00.

4.2.4.14. 4-((4-(Benzylamino)-5-carbamoylpyrimidin-2-yl)amino)-2-(dimethylamino)phenyl methane sulfonate (5n). Refer to general procedure for the synthesis of 5n, as described in section 4.1.4. 46.8% isolated yield; white solid. 1H NMR (DMSO- d_6 , 400 MHz) δ ppm 2.67 (s, 6H), 3.32 (s, 3H), 4.72 (d, $J = 5.6$ Hz, 2H), 7.05 (d, $J = 8.8$ Hz, 1H), 7.23-7.29 (m, 2H), 7.33-7.36 (m, 4H), 7.57 (s, 1H), 8.57 (s, 1H), 9.55 (s, 2H). ^{13}C NMR (DMSO- d_6 , 100 MHz) δ ppm 37.4, 42.9, 44.2, 100.9, 107.7, 108.4, 127.1, 127.9, 128.5, 130.4, 140.0, 140.2, 143.8, 157.3, 160.7, 161.4, 169.2. ESI-MS: m/z Calcd for $C_{21}H_{25}N_6O_4S$ 456.52 $[M]^+$, found 456.90.

4.2.4.15. 4-((4-(Benzylamino)-5-carbamoylpyrimidin-2-yl)amino)-2-carbamoylphenyl methane sulfonate (5o). Refer to general procedure for the synthesis of 5o, as described in section 4.1.4. 48.5% isolated yield; white solid. 1H NMR (DMSO- d_6 , 400 MHz) δ ppm 2.05 (s, 3H), 3.33 (s, 3H), 4.71 (d, $J = 6.0$ Hz, 2H), 7.26-7.19 (m, 6H), 7.47 (d, $J = 7.6$ Hz, 1H), 8.31 (s, 1H), 8.57 (s, 1H), 9.50 (s, 1H), 9.54 (s, 1H), 9.67 (s, 1H). ^{13}C NMR (DMSO- d_6 , 100 MHz) δ ppm 23.8, 38.1, 43.9, 100.7, 109.1, 116.2, 123.1, 127.2, 127.5, 128.8, 131.2, 139.6, 139.8, 142.0, 157.7, 160.3, 161.9, 163.2, 169.4. ESI-MS: m/z Calcd for $C_{21}H_{23}N_6O_5S$ $[M+1]^+$ 471.50, found 471.19.

4.2.5. Preparation of ethyl 4-hydroxy-2-((4-((methylsulfonyl)oxy)phenyl)amino)pyrimidine-5-carboxylate (7)

Ethyl 4-hydroxy-2-(methylthio)pyrimidine-5-carboxylate (6; 10 g; 46.7 mmol) was dissolved in a mixture of dioxan and chloroform (1:1; 262 mL). Reaction mixture was cooled up to $-2^\circ C$, treated with m-CPBA (60%; 20.14 g, 70.0 mmol) and stirred for 50 min at $0^\circ C$. Reaction mixture was quenched by 10% aq. sodium metabisulfite (262 mL), extracted with chloroform and washed with aq. 10% sodium bicarbonate. The organic layer was dried over sodium sulfate (40 g) and the solvent was evaporated under reduced pressure to obtain ethyl 4-hydroxy-2-(methylsulfinyl)pyrimidine-5-carboxylate as a white solid (8.6 g, 80%), which was further used in the next step without

purification.

To the mixture of ethyl 4-hydroxy-2-(methylsulfinyl)pyrimidine-5-carboxylate (8.6 g; 37.4 mmol) and PTSA (7.82 g; 41.1 mmol), dissolved in NMP (80 mL) was added 4-(methylsulfonyl)aniline (6.99 g; 37.4 mmol), at RT. The reaction mixture was heated at 100-110 °C for 1-2 h. After completion of reaction, the mixture was diluted with water and the compound was extracted in EtOAc. Organic layer was dried over sodium sulfate, filtered and concentrated under vacuum to afford the crude product. Crude product was purified by flash chromatography over silica gel (100-200 mesh) with 2% MeOH/CHCl₃ to get the ethyl 4-hydroxy-2-((4-((methylsulfonyl)oxy)phenyl)amino)pyrimidine-5-carboxylate (7) (9.9 g, 75%). ¹H NMR (DMSO-*d*₆, 400 MHz) δ ppm 1.26 (t, *J* = 7.0 Hz, 3H), 3.48 (s, 3H), 4.20 (q, *J* = 6.8 Hz, 2H), 6.57 (d, *J* = 9.2 Hz, 2H), 7.34 (d, *J* = 8.8 Hz, 2H), 8.49 (s, 1H), 9.75 (s, 1H), 11.25 (s, 1H); ESI-MS: *m/z* Calcd for C₁₄H₁₆N₃O₅S [M+1]⁺ 354.35, found 354.58.

4.2.6. 4-hydroxy-2-((4-((methylsulfonyl)oxy)phenyl)amino)pyrimidine-5-carboxylic acid (8)

Ethyl 4-hydroxy-2-((4-((methylsulfonyl)oxy)phenyl)amino)pyrimidine-5-carboxylate (7; 9.0 g, 25.5 mmol) was dissolved in THF (90 mL). LiOH (3.05 g, 127 mmol) dissolved in water (5 mL) was added in to the reaction mixture and stirred overnight at 25 °C. After completion of reaction, the reaction mixture was concentrated by rotary evaporation to remove excess THF. Mixture was acidified (10 M HCl to pH ~ 5), which led to the formation of a white precipitate. The solid compound filtered, washed with water and dried under vacuum to afford 4-hydroxy-2-((4-((methylsulfonyl)oxy)phenyl)amino)pyrimidine-5-carboxylic acid (8), as a white solid. (6.63 g, 80%). ¹H NMR (DMSO-*d*₆, 400 MHz) δ ppm 3.56 (s, 3H), 7.37 (d, *J* = 8.8 Hz, 2H), 7.67 (d, *J* = 8.8 Hz, 2H), 8.51 (s, 1H), 9.85 (s, 1H). ESI-MS: *m/z* Calcd for C₁₂H₁₂N₃O₆S [M+1]⁺ 326.30, found 326.01.

4.2.7. 4-((5-carbamoyl-4-hydroxypyrimidin-2-yl)amino)phenyl methanesulfonate (9)

4-Hydroxy-2-((4-((methylsulfonyl)oxy)phenyl)amino)pyrimidine-5-carboxylic acid (8; 6.0 g, 18.44 mmol) was dissolved in DMF (50 mL) and treated with HOBt (2.82 g; 18.44 mmol) and EDC.HCl (7.07 g; 36.9 mmol), at RT. After stirring 1 hr., aq. Ammonia (20 mL) was added at 0 °C and stirred for 1 hr., at RT. The reaction mixture was quenched with water (200 mL) which resulted in the formation of a white precipitate. The solid compound was filtered, washed with water and dried under reduced pressure to afford 4-((5-carbamoyl-4-hydroxypyrimidin-2-yl)amino)phenyl methanesulfonate (9; 4.19 g, 70%). ¹H NMR (DMSO-*d*₆, 400 MHz) δ ppm 3.33 (s, 3H), 7.21 (d, *J* = 8.8 Hz, 2H), 7.87 (d, *J* = 8.8 Hz, 2H), 8.37 (s, 1H), 9.33 (s, 1H), 17.6 (s, 1H). ESI-MS: *m/z* Calcd for C₁₂H₁₃N₄O₅S [M+2]⁺ 324.31, found 326.05.

4.2.8. 4-((5-carbamoyl-4-chloropyrimidin-2-yl)amino)phenyl methanesulfonate (10)

To a solution of 4-((5-carbamoyl-4-hydroxypyrimidin-2-yl)amino)phenyl methanesulfonate (9; 4.0 g, 12.33 mmol), in toluene (50 mL) was added DIPEA (2.6 mL, 14.8 mmol) and POCl₃ (2.3 mL, 24.67 mmol) drop wise, at 0-5 °C. The reaction mixture was refluxed for 2 hr. After completion of reaction, mixture was cooled to RT, quenched with ice - water (180 mL) to afford white precipitate. The precipitated compound was filtered, washed with cold water to get 4-((5-carbamoyl-4-chloropyrimidin-2-yl)amino)phenyl methanesulfonate (10; 2.96 g, 70%). ¹H NMR (DMSO-*d*₆, 400 MHz) δ ppm 3.37 (s, 3H), 7.34 (d, *J* = 9.2 Hz, 2H), 7.80 (d, *J* = 9.2 Hz, 2H), 8.92 (s, 1H), 10.70 (s, 1H). ESI-MS: *m/z* Calcd for C₁₂H₁₂ClN₄O₄S [M+1]⁺ 343.75, found 343.80.

4.2.9. General procedure for the synthesis of compound 11a-o

4-((5-carbamoyl-4-chloropyrimidin-2-yl)amino)phenyl methanesulfonate (10; 1.0 eq) was dissolved in dioxane (40 mL) and DIPEA

(1.1 eq) was added to the reaction mixture at 0 °C followed by the addition of different amines (1.0 eq). The reaction mixture was stirred at 0 °C for 6 hr. After completion of reaction, the mixture was diluted with water and the compound was extracted in EtOAc. Organic layer was dried over sodium sulfate, filtered and concentrated under vacuum to afford the crude product. Crude product was purified by flash chromatography over silica gel (100-200 mesh), with 2% MeOH/CHCl₃ to provide the desired title product (11a-o).

4.2.9.1. 4-((4-Amino-5-carbamoylpyrimidin-2-yl)amino)phenyl methanesulfonate (11a). Refer to the general procedure for the synthesis of 11a, as described in section 4.1.9. 49.4% isolated yield; white solid. ¹H NMR (DMSO-*d*₆, 400 MHz) δ ppm 3.33 (s, 3H), 7.22 (d, *J* = 9.2 Hz, 2H), 7.89 (d, *J* = 9.2 Hz, 2H), 8.54 (s, 1H), 9.58 (s, 1H). ¹³C NMR (DMSO-*d*₆, 100 MHz) δ ppm 37.4, 100.1, 120.8, 122.3, 140.2, 142.9, 155.1, 158.2, 160.5, 161.8. ESI-MS: *m/z* Calcd for C₁₂H₁₃N₅O₄S [M]⁺ 323.33, found 323.80.

4.2.9.2. 4-((5-Carbamoyl-4-(cyclopropylamino)pyrimidin-2-yl)amino)phenyl methanesulfonate (11b). Refer to the general procedure for the synthesis of 11b, as described in section 4.1.9. 48.9% isolated yield; white solid. ¹H NMR (DMSO-*d*₆, 400 MHz) δ ppm 0.54 (t, *J* = 3.0 Hz, 2H), 0.84 (t, *J* = 3.4 Hz, 2H), 2.66-2.67 (m, 1H), 3.32 (s, 3H), 7.26 (d, *J* = 9.2 Hz, 2H), 8.02 (d, *J* = 8.8 Hz, 2H), 8.53 (s, 1H), 9.22 (s, 1H), 9.75 (s, 1H). ¹³C NMR (DMSO-*d*₆, 100 MHz) δ ppm 7.5, 25.0, 37.1, 100.5, 121.0, 122.5, 140.5, 144.0, 158.2, 160.4, 161.8, 169.4. ESI-MS: *m/z* Calcd for C₁₅H₁₈N₅O₄S [M+1]⁺ 364.39, found 364.00.

4.2.9.3. 4-((5-Carbamoyl-4-(cyclobutylamino)pyrimidin-2-yl)amino)phenyl methane sulfonate (11c). Refer to the general procedure for the synthesis of 11c, as described in section 4.1.9. 49.7% isolated yield; white solid. ¹H NMR (DMSO-*d*₆, 400 MHz) δ ppm 1.25 (m, 2H), 1.78 (m, 2H), 2.37 (m, 2H), 3.33 (s, 3H), 4.51-4.55 (m, 1H), 7.28 (d, *J* = 9.2 Hz, 2H), 7.87 (d, *J* = 9.2 Hz, 2H), 8.53 (s, 1H), 9.30 (d, *J* = 7.2 Hz, 1H), 9.67 (s, 1H). ¹³C NMR (DMSO-*d*₆, 100 MHz) δ ppm 12.5, 30.2, 37.3, 51.2, 100.8, 121.5, 122.3, 140.1, 144.5, 158.8, 160.9, 161.7, 169.3. ESI-MS: *m/z* Calcd for C₁₆H₂₀N₅O₄S [M+1]⁺ 378.42, found 378.00.

4.2.9.4. 4-((5-Carbamoyl-4-(cyclopentylamino)pyrimidin-2-yl)amino)phenylmethane sulfonate (11d). Refer to the general procedure for the synthesis of 11d, as described in section 4.1.9. 48.2% isolated yield; white solid. ¹H NMR (DMSO-*d*₆, 400 MHz) δ ppm 1.46-1.49 (m, 2H), 1.50-1.73 (m, 4H), 1.98-2.06 (m, 2H), 3.32 (s, 3H), 4.30-4.38 (m, 1H), 7.25 (d, *J* = 9.2 Hz, 2H), 7.88 (d, *J* = 9.2 Hz, 2H), 8.52 (s, 1H), 9.20 (d, *J* = 7.2 Hz, 1H), 9.65 (s, 1H). ¹³C NMR (DMSO-*d*₆, 100 MHz) δ ppm 23.8, 33.2, 37.5, 52.0, 100.2, 120.4, 122.6, 140.1, 143.5, 157.5, 160.2, 161.4, 169.5. ESI-MS: *m/z* Calcd for C₁₇H₂₂N₅O₄S [M+1]⁺ 392.45, found 392.00.

4.2.9.5. 4-((5-Carbamoyl-4-(cyclohexylamino)pyrimidin-2-yl)amino)phenylmethanes sulfonate (11e). Refer to the general procedure for the synthesis of 11e, as described in section 4.1.9. 47.5% isolated yield; white solid. ¹H NMR (DMSO-*d*₆, 400 MHz) δ ppm 1.24-1.31 (m, 3H), 1.35-1.44 (m, 2H), 1.62-1.59 (m, 1H), 1.70-1.73 (m, 2H), 1.95-1.98 (m, 2H), 3.33 (s, 3H), 3.93-3.94 (m, 1H), 7.25 (d, *J* = 9.2 Hz, 2H), 7.86 (d, *J* = 8.8 Hz, 2H), 8.52 (s, 1H), 9.17 (d, *J* = 7.2 Hz, 1H), 9.66 (s, 1H). ¹³C NMR (DMSO-*d*₆, 100 MHz) δ ppm 24.8, 25.7, 32.6, 37.5, 49.0, 100.0, 120.3, 122.6, 140.1, 143.5, 157.7, 160.3, 161.0, 169.6. ESI-MS: *m/z* Calcd for C₁₈H₂₄N₅O₄S [M+1]⁺ 406.47, found 406.00.

4.2.9.6. 4-((5-Carbamoyl-4-(cyclopentylmethyl)amino)pyrimidin-2-yl)amino)phenylmethane sulfonate (11f). Refer to the general procedure for the synthesis of 11f, as described in section 4.1.9. 48.2% isolated yield; white solid. ¹H NMR (DMSO-*d*₆, 400 MHz) δ ppm 1.18-1.22 (m, 2H), 1.53-1.55 (m, 2H), 1.56-1.60 (m, 2H), 1.62-1.75 (m, 2H),

1.98-2.00 (m, 1H), 3.51 (s, 5H), 7.28 (d, $J = 8.8$ Hz, 2H), 7.85 (d, $J = 8.0$ Hz, 2H), 8.51 (s, 1H), 9.40 (s, 1H), 9.85 (s, 1H). ^{13}C NMR (DMSO- d_6 , 100 MHz) δ ppm 25.2, 30.3, 37.5, 45.3, 100.5, 120.9, 122.8, 139.4, 143.9, 158.9, 159.4, 161.8, 169.1. ESI-MS: m/z Calcd for $\text{C}_{18}\text{H}_{24}\text{N}_5\text{O}_4\text{S}$ $[\text{M} + 1]^+$ 406.47, found 406.30.

4.2.9.7. 4-((5-Carbamoyl-4-(isobutylamino)pyrimidin-2-yl)amino)phenyl methane sulfonate (11g). Refer to the general procedure for the synthesis of 11g, as described in section 4.1.9. 46.3% isolated yield; white solid. ^1H NMR (DMSO- d_6 , 400 MHz) δ ppm 0.93 (d, $J = 6.8$ Hz, 6H), 3.10 (s, 2H), 3.33 (s, 3H), 4.10-4.15 (m, 1H), 7.25 (d, $J = 9.2$ Hz, 2H), 7.87 (d, $J = 9.2$ Hz, 2H), 8.53 (s, 1H), 9.38 (s, 1H), 9.66 (s, 1H). ^{13}C NMR (DMSO- d_6 , 100 MHz) δ ppm 21.3, 29.9, 37.4, 49.2, 100.1, 121.2, 122.0, 139.6, 144.0, 159.0, 159.9, 161.9, 169.4. ESI-MS: m/z Calcd for $\text{C}_{16}\text{H}_{21}\text{N}_5\text{O}_4\text{S}$ $[\text{M}]^+$ 379.44, found 379.50.

4.2.9.8. 4-((5-Carbamoyl-4-((3-methylbutan-2-yl)amino)pyrimidin-2-yl)amino)phenyl methane sulfonate (11h). Refer to the general procedure for the synthesis of 11h, as described in section 4.1.9. 48.1% isolated yield; white solid. ^1H NMR (DMSO- d_6 , 400 MHz) δ ppm 0.90 (d, $J = 6.8$ Hz, 3H), 0.94 (d, $J = 6.8$ Hz, 3H), 1.13 (d, $J = 6.8$ Hz, 3H), 1.85-1.90 (m, 1H), 3.34 (s, 3H), 4.06-4.11 (m, 1H), 7.26 (d, $J = 9.2$ Hz, 2H), 7.85 (d, $J = 9.2$ Hz, 2H), 8.53 (s, 1H), 9.27 (d, $J = 8.4$ Hz, 3H), 9.65 (s, 1H). ^{13}C NMR (DMSO- d_6 , 100 MHz) δ ppm 16.6, 18.0, 18.4, 31.9, 37.1, 50.1, 99.5, 119.9, 122.2, 139.6, 143.1, 157.1, 159.8, 161.0, 169.2. ESI-MS: m/z Calcd for $\text{C}_{17}\text{H}_{24}\text{N}_5\text{O}_4\text{S}$ $[\text{M} + 1]^+$ 394.46, found 394.20.

4.2.9.9. (R)-4-((5-Carbamoyl-4-((3-methylbutan-2-yl)amino)pyrimidin-2-yl)amino) phenyl methane sulfonate (11i). Refer to the general procedure for the synthesis of 11i, as described in section 4.1.9. 47.4% isolated yield; white solid. ^1H NMR (DMSO- d_6 , 400 MHz) δ ppm 0.90 (d, $J = 6.8$ Hz, 3H), 0.94 (d, $J = 6.8$ Hz, 3H), 1.13 (d, $J = 6.4$ Hz, 3H), 1.84-1.92 (m, 1H), 3.34 (s, 3H), 4.05-4.12 (m, 1H), 7.26 (d, $J = 9.2$ Hz, 2H), 7.87 (d, $J = 9.2$ Hz, 1H), 8.54 (s, 1H), 9.28 (d, $J = 8.4$ Hz, 2H), 9.64 (s, 1H). ^{13}C NMR (DMSO- d_6 , 100 MHz) δ ppm 17.1, 18.4, 18.8, 32.4, 37.5, 50.6, 100.0, 120.3, 122.6, 140.0, 143.5, 157.7, 160.3, 161.5, 169.7. ESI-MS: m/z Calcd for $\text{C}_{17}\text{H}_{24}\text{N}_5\text{O}_4\text{S}$ $[\text{M} + 1]^+$ 394.46, found 394.14.

4.2.9.10. (S)-4-((5-Carbamoyl-4-((3-methylbutan-2-yl)amino)pyrimidin-2-yl)amino) phenyl methane sulfonate (11j). Refer to the general procedure for the synthesis of 11j, as described in section 4.1.9. 47.4% isolated yield; white solid. ^1H NMR (DMSO- d_6 , 400 MHz) δ ppm 0.88 (d, $J = 6.8$ Hz, 3H), 0.94 (d, $J = 6.8$ Hz, 3H), 1.12 (d, $J = 6.8$ Hz, 3H), 1.85-1.89 (m, 1H), 3.33 (s, 1H), 4.06-4.11 (m, 1H), 7.26 (d, $J = 9.2$ Hz, 2H), 7.85 (d, $J = 9.2$ Hz, 2H), 8.52 (s, 1H), 9.27 (d, $J = 8.4$ Hz, 1H), 9.64 (s, 1H). ^{13}C NMR (DMSO- d_6 , 100 MHz) δ ppm 16.9, 18.1, 18.6, 32.1, 37.3, 50.2, 100.1, 120.1, 122.3, 140.1, 143.4, 157.5, 160.0, 161.2, 169.5. ESI-MS: m/z Calcd for $\text{C}_{17}\text{H}_{24}\text{N}_5\text{O}_4\text{S}$ $[\text{M} + 1]^+$ 394.46, found 394.20.

4.2.9.11. (R)-4-((5-Carbamoyl-4-((1-phenylethyl)amino)pyrimidin-2-yl)amino)phenyl methane sulfonate (11k). Refer to the general procedure for the synthesis of 11k, as described in section 4.1.9. 47.8% isolated yield; white solid. ^1H NMR (DMSO- d_6 , 400 MHz) δ ppm 1.48 (d, $J = 8.2$ Hz, 3H), 3.32 (s, 3H), 5.20-5.23 (m, 1H), 7.21-7.16 (m, 3H), 7.23-7.42 (m, 4H), 7.60-7.66 (m, 2H), 8.55 (s, 1H), 9.63 (m, 2H). ^{13}C NMR (DMSO- d_6 , 100 MHz) δ ppm 20.9, 37.4, 55.2, 100.4, 121.1, 122.7, 127.1, 127.9, 128.7, 139.7, 140.3, 143.9, 158.5, 160.8, 162.2, 169.8. ESI-MS: m/z Calcd for $\text{C}_{20}\text{H}_{21}\text{N}_5\text{O}_4\text{S}$ $[\text{M}]^+$ 427.48, found 427.80.

4.2.9.12. 4-((5-Carbamoyl-4-((3-fluorobenzyl)amino)pyrimidin-2-yl)amino)phenyl methane sulfonate (11l). Refer to the general procedure for the synthesis of 11l, as described in section 4.1.9. 46.2% isolated yield; white solid. ^1H NMR (DMSO- d_6 , 400 MHz) δ ppm 3.33 (s, 3H),

4.67 (d, $J = 6.0$ Hz, 2H), 7.04-7.19 (m, 5H), 7.35-7.41 (m, 1H), 7.68 (d, $J = 9.2$ Hz, 2H), 8.57 (s, 1H), 9.59 (t, $J = 5.6$ Hz, 2H), 9.68 (s, 1H). ^{13}C NMR (DMSO- d_6 , 100 MHz) δ ppm 37.6, 43.7, 100.3, 112.5, 117.9, 121.1, 122.8, 123.1, 127.0, 139.5, 142.1, 143.8, 158.2, 159.9, 160.9, 162.0, 169.6. ESI-MS: m/z Calcd for $\text{C}_{19}\text{H}_{18}\text{FN}_5\text{O}_4\text{S}$ $[\text{M}] + 431.44$, found 431.80.

4.2.9.13. 4-((5-Carbamoyl-4-((4-fluorobenzyl)amino)pyrimidin-2-yl)amino)phenyl methane sulfonate (11m). Refer to the general procedure for the synthesis of 11m, as described in section 4.1.9. 47.3% isolated yield; white solid. ^1H NMR (DMSO- d_6 , 400 MHz) δ ppm 3.32 (s, 3H), 4.67 (d, $J = 6.0$ Hz, 2H), 7.15-7.20 (m, 4H), 7.35-7.39 (m, 2H), 7.72 (d, $J = 8.8$ Hz, 2H), 8.56 (s, 1H), 9.55 (s, 1H), 9.67 (s, 1H). ^{13}C NMR (DMSO- d_6 , 100 MHz) δ ppm 37.5, 43.4, 100.5, 115.2, 121.0, 122.5, 127.7, 139.2, 140.3, 143.2, 159.4, 160.2, 160.8, 162.3, 169.1. ESI-MS: m/z Calcd for $\text{C}_{19}\text{H}_{18}\text{FN}_5\text{O}_4\text{S}$ $[\text{M}] + 431.44$, found 431.90.

4.2.9.14. 4-((5-Carbamoyl-4-((2-fluorobenzyl)amino)pyrimidin-2-yl)amino)phenyl methane sulfonate (11n). Refer to the general procedure for the synthesis of 11n, as described in section 4.1.9. 47.9% isolated yield; white solid. ^1H NMR (DMSO- d_6 , 400 MHz) δ ppm 3.32 (s, 3H), 4.67 (d, $J = 6$ Hz, 2H), 7.13-7.17 (m, 3H), 7.21-7.33 (m, 3H), 7.69 (d, $J = 8.8$ Hz, 2H), 8.57 (s, 1H), 9.55 (s, 1H), 9.67 (s, 1H). ^{13}C NMR (DMSO- d_6 , 100 MHz) δ ppm 37.2, 39.3, 100.6, 114.7, 121.4, 122.8, 124.0, 128.1, 129.5, 139.0, 139.2, 143.5, 159.2, 160.5, 161.2, 162.9, 169.7. ESI-MS: m/z Calcd for $\text{C}_{19}\text{H}_{18}\text{FN}_5\text{O}_4\text{S}$ $[\text{M}]^+$ 431.44, found 431.90.

4.2.9.15. 4-((5-Carbamoyl-4-((naphthalen-1-ylmethyl)amino)pyrimidin-2-yl)amino) phenyl methane sulfonate (11o). Refer to the general procedure for the synthesis of 11o, as described in section 4.1.9. 50.5% isolated yield; white solid. ^1H NMR (DMSO- d_6 , 400 MHz) δ ppm 1.67 (d, $J = 6.8$ Hz, 3H), 3.28 (s, 3H), 6.05 (t, $J = 6.4$ Hz, 1H), 6.52-6.58 (m, 2H), 7.36-7.44 (m, 2H), 7.45-7.48 (m, 2H), 7.64-7.85 (m, 2H), 7.89-7.91 (m, 1H), 8.01 (d, $J = 8.0$ Hz, 1H), 8.27 (d, $J = 8.4$ Hz, 1H), 8.59 (s, 1H), 8.97 (s, 1H), 9.83 (s, 1H), 12.90 (d, $J = 9.2$ Hz, 1H). ^{13}C NMR (DMSO- d_6 , 100 MHz) δ ppm 21.5, 37.6, 57.9, 100.2, 121.8, 122.4, 122.9, 125.8, 126.9, 128.1, 131.0, 139.4, 140.9, 143.5, 159.7, 161.0, 162.7, 169.2. ESI-MS: Calcd for $\text{C}_{24}\text{H}_{25}\text{N}_5\text{O}_4\text{S}$ $[\text{M} + 2]^+$ 477.54, found 479.21.

4.3. In vitro and ex vivo assay

4.3.1. Enzymatic potency of JAK inhibitors (biochemical assay)

Human JAK1-3 and TYK2 kinase domains were purchased from Carna Biosciences (Japan), and the assay was performed using a streptavidin-coated 96-well plate. The reaction mixture contained 15 mM Tris-HCl (pH 7.5), 0.01% Tween 20, 2 mM DTT, 10 mM MgCl_2 , 250 nM Biotin-Lyn-Substrate-2 (Peptide Institute, Inc., Osaka, Japan) and ATP. The final concentrations of ATP were 10 μM for JAK1-3 and TYK2. Test compounds were dissolved in DMSO and the reaction was initiated by adding the kinase domain, followed by incubation at room temperature for 1 hr. Kinase activity was measured as the rate of phosphorylation of Biotin-Lyn-Substrate-2, using HRP-conjugated anti-phosphotyrosine antibody (HRP-PY-20; Santa Cruz Biotechnology, CA, USA) with a phosphotyrosine-specific ELISA. All the experiments were performed in duplicate. The IC_{50} values were calculated using linear regression analysis [32].

4.3.2. JAK cellular assays using human peripheral blood mononuclear cells (PBMCs)

PBMCs were collected from healthy volunteers (as per Zydus Research Centre, ethical committee protocol), into sodium heparin vacutainer tubes. After incubation with compound 11i and Tofacitinib at

37 $^\circ\text{C}$ for 30 min, blood was triggered with either recombinant human IL-6 (400 ng/mL; R&D Systems), IL-2 (20 ng/mL; R&D Systems),

GM-CSF (100 ng/mL; Pepro-Tech), or vehicle (PBS plus 0.1% [w/v] BSA), at 37 °C for 20 min and treated with pre-warmed 13 lysis/fix buffer (BD Biosciences) to lyse RBCs and fix leukocytes. Cells were permeabilized with 100% MeOH and incubated with anti-pSTAT3 and anti-CD4 (IL-6-triggered samples), anti-pSTAT5 and anti-CD4 Abs (IL-2-triggered samples), or anti-pSTAT5 Abs (GM-CSF-triggered samples; all Abs were from BD Biosciences) at 4 °C, for 30 min, washed once with PBS and analyzed on a FACS Canto II flow cytometer. [33,34] IC₅₀ values were determined, using Prism software (Version 7, GraphPad), for Tofacitinib and 11i, Table 4.

4.3.3. Plasma protein binding

An equilibrium dialysis method was used to determine the plasma fraction unbound (fu) values. Briefly, dialysis membranes (MWCO 12-14 K) and 96-well dialysis devices were assembled following the manufacturer's instructions (HT Dialysis, LLC, USA). Human plasma samples containing 1 μmol/L test compounds with 1% DMSO were dialyzed against PBS for 6 h in a humidified incubator (75% relative humidity; 5% CO₂/95% air) at 37 °C at 450 RPM. Quadruplicates of binding were measured for each compound. Samples were matrix-matched and quenched with cold acetonitrile containing internal standard(s). The solutions were centrifuged and the supernatant was analyzed using LC-MS/MS.

4.4. In vivo efficacy studies

The animal experiments were carried out in rats and mice, bred in-house. Animals were housed in groups of 6 animals per cage, for a week, in order to habituate them to vivarium conditions (25 ± 4 °C, 60-65% relative humidity, 12:12 h light dark cycle, with lights on, at 7.30 am). All the animal experiments were carried out according to the internationally valid guidelines following approval by the 'Zydus Research Center, animal ethical committee'.

4.4.1. Protocol for collagen induced arthritis (CIA) study in mice

CIA study is a representative animal model of human rheumatoid arthritis [35]. Following 7 days acclimation, male DBA1j (8 to 12-weeks old) mice were randomly assigned to groups according body weight. Mice were immunized subcutaneously in the tail using bovine type II collagen mix in complete Freund's adjuvant (CFA). Twenty-one days after the first immunization, mice were given booster dose of collagen in incomplete Freund's adjuvant (IFA). Mice were monitored every other day after the booster dose for the development of arthritis. Mice were recruited for the study once clinical signs were visible. Eight animals were assigned each of three groups [vehicle, Tofacitinib and test compound, 11i], treatment was continued for three weeks and percentage inhibition in clinical score is recorded as per graded score. Body weights of the animals were also recorded 3 times a week as a measure of treatment related side effect and paw thickness measured twice a week (Fig. 2a). The mice were scored in a blinded manner, for signs of arthritis in each paw according to the following scale: 0 - no swelling or redness/normal paw; 1- swelling and/or redness in one digit; 2- swelling and/or redness in two or more digits; and 3- entire paw is swollen or red. The severity score was reported as the sum of all four paws for each mouse and expressed as the average severity score for each group.

4.4.2. Protocol for adjuvant induced arthritis (AIA) model in rats

Arthritis was induced in female Lewis rats by inoculation with Freund's complete adjuvant (CFA) [36]. Briefly, on day 0, rats were anesthetized (mixture of ketamine and xylazine (80: 10 mg/kg, intraperitoneally)) and then injected with 0.1 mL CFA (1 mg/mL of heat-inactivated Mycobacterium tuberculosis) intra-dermally, at the base of the tail. Eight animals were assigned in each of the three groups [vehicle (2% sodium carboxymethylcellulose (CMC), positive control (Tofacitinib, 60 mg/kg) and test compound 11i (3, 10 and 30 mg/kg)]. Treatment was continued for 20 days (once daily, by oral gavage) and

paw edema determined by measuring changes in the paw volume, using a plethysmometer, on days 10, 12, 14, 16, 18 and 20, post- CFA injection. Statistical analysis was performed by one-way ANOVA (Dunnett's method, data represent the mean ± S.E.M., n = 8/group).

4.5. Pharmacokinetic studies

A comparative single dose (3 mg/kg, po and 1 mg/kg, iv) PK study of compounds 5k, 11i and Tofacitinib was evaluated in overnight fasted male C57BL/6J mice (n = 6). Serial blood samples were collected in the micro-centrifuge tubes containing EDTA, at pre-dose, 0.15, 0.3, 0.5, 0.75, 1, 2, 4, 6, 8, 24 and 30 h post-dose, after the compounds administration. Approximately 0.3 mL of blood was collected at each time points and centrifuged at 4 °C. The obtained plasma was frozen, stored at -70 °C and the concentrations of compounds in plasma were determined by the LC-MS/MS (Shimadzu LC10AD, USA), using YMC hydrosphere C18 (2.0 × 50 mm, 3 μm) column (YMC Inc., USA). The pharmacokinetic parameters, such as T_{max}, t_{1/2}, C_{max}, AUC and %F were calculated using a non-compartmental model of WinNonlin software version 5.2.1.

4.6. Docking studies

Multiple structures of JAK3, co-crystallized with various ligands, were analyzed, and the structure with PDB ID 5W86 (solved at 2.6 Å) was selected due to core similarity of the co-crystallized ligand and Cerdulatinib [37]. The protein was prepared using protein preparation wizard of Schrodinger Suite 2018-4, at pH 7.4. Ligands were prepared using Ligprep module at pH 7.0 ± 0.5, with default settings. Glide grid was used with default options for grid generation and Glide SP docking was used for docking simulation with default settings. The docked pose of Cerdulatinib, 5k and 11i was analyzed with respect to docking score, docking pose and hydrogen bonding interactions with the key region residues of the JAK3 enzyme.

Acknowledgments

Authors thank the management of Zydus Research Centre (ZRC), Cadila Healthcare Ltd. for support and encouragement and the analytical department for providing analytical data.

Declaration of Competing Interest

The authors declare no competing financial interest.

Appendix A. Supplementary data

Supplementary data to this article can be found online at <https://doi.org/10.1016/j.bioorg.2020.103851>.

References

- [1] D. Boyle, H. Kim, K. Topolewski, B. Bartok, G. Firestein, Novel phosphoinositide 3-kinase δ, γ inhibitor: potent anti-inflammatory effects and joint protection in models of rheumatoid arthritis, *J. Pharmacol. Exp. Ther.* 348 (2014) 271-280, <https://doi.org/10.1124/jpet.113.205955>.
- [2] P. Conigliaro, P. Triggianese, E. Martino, M. Chimenti, F. Sunzini, A. Viola, Claudia, Challenges in the treatment of Rheumatoid Arthritis, *Autoimmun. Rev.* 18 (2019) 706-713, <https://doi.org/10.1016/j.autrev.2019.05.007>.
- [3] R. Roskoski, *Pharmacol. Res.* 111 (2016) 784-803, <https://doi.org/10.1016/j.phrs.2016.07.038>.
- [4] C. Schindler, C. Plumlee, Interferons pen the JAK-STAT pathway, *Seminars Cell Dev. Biol.* 19 (2008) 311-318, <https://doi.org/10.1016/j.semcdb.2008.08.010>.
- [5] A. Mohr, N. Chatain, T. Domszalai, N. Rinis, M. Sommerauer, M. Vogt, G. Muller-Newen, Dynamics and non-canonical aspects of JAK/STAT signaling, *Eur. J. Cell Biol.* 91 (2012) 524-532, <https://doi.org/10.1016/j.ejcb.2011.09.005>.
- [6] J. John, D. Schwartz, A. Villarino, M. Gadina, I. McInnes, A. Laurence, The JAK-STAT pathway: impact on human disease and therapeutic, *Annu. Rev. Med.* 66 (2015) 311-328, <https://doi.org/10.1146/annurev-med-051113-024537>.
- [7] N. Sailliet, C. Brosseau, J. Robert, S. Brouard, Role of JAK inhibitors and immune

- cells in transplantation, *Cytokine Growth Factor Rev.* 47 (2019) 62-63, <https://doi.org/10.1016/j.cytogfr.2019.05.002>.
- [8] H. Hammaren, A. Virtanen, J. Raivola, O. Silvennoinen, The regulation of JAKs in cytokine signaling and its breakdown in disease, *Cytokine* 118 (2019) 48-63, <https://doi.org/10.1016/j.cyto.2018.03.041>.
- [9] Z. Yan, S. Gibson, J. Buckley, H. Qin, E. Benveniste, Role of JAK/STAT signaling pathway in regulation of innate immunity in neuroinflammatory diseases, *Clin. Immunol.* 189 (2018) 4-13, <https://doi.org/10.1016/j.clim.2016.09.014>.
- [10] C. Haan, S. Kreis, C. Mague, I. Behrmann, Jaks and Cytokine receptors - An intimate relationship, *Biochem. Pharmacol.* 72 (2006) 1538-1546, <https://doi.org/10.1016/j.bcp.2006.04.013>.
- [11] K. Yamaoka, P. Saharinen, M. Pesu, V. Holt, O. Silvennoinen, J. John, The Janus Kinases (JAKs), *Genome Biol.* 5 (2004) 253, <https://doi.org/10.1186/GB-2004-5-12-253>.
- [12] M. Flanagan, T. Blumenkopf, W. Brissette, M. Brown, J. Casavant, C. Shang-Poa, J. Doty, E. Elliott, M. Fisher, M. Hines, C. Kent, E. Kudlacz, B. Lillie, K. Magnuson, S. McCurdy, M. Munchhof, B. Perry, P. Sawyer, T. Strelevitz, C. Subramanyam, J. Sun, D. Whipple, P. Changelian, Discovery of CP-690,550: Apotent and selective Janus Kinase (JAK) inhibitor for the treatment of Autoimmune Diseases and Organ Transplant Rejection, *J. Med. Chem.* 53 (2010) 8468-8484, <https://doi.org/10.1021/jm1004286>.
- [13] N. Elliott, S. Cleveland, V. Grann, J. Janik, T. Waldmann, U. Dave, FERM domain mutations induce gain of function in JAK3 in adult T-Cell leukemia/lymphoma, *Blood.* 118 (2011) 3911-3921, <https://doi.org/10.1182/blood-2010-12-319467>.
- [14] M. Chen, A. Cheng, Y. Chen, A. Hymel, E. Hanson, L. Kimmel, Y. Minami, T. Taniguchi, P. Changelian, J. John, The amino terminus of JAK3 is necessary and sufficient for binding to the common γ Chain and confers the ability to transmit interleukin 2- mediated signals, *Immunology* 94 (1997) 6910-6915, <https://doi.org/10.1073/pnas.94.13.6910>.
- [15] M. Genovese, J. Slomen, M. Weinblatt, G. Burmester, S. Meerwein, H. Camp, L. Wang, A. Othman, N. Khan, A. Pangan, S. Jungerwirth, Efficacy and safety of ABT-494, a Selective JAK-1 inhibitor, in a Phase IIb study in Patients with Rheumatoid Arthritis and an Inadequate Response to Methotrexate, *Arthritis Rheumatol.* 68 (2016) 2857-2866, <https://doi.org/10.1002/art.39808>.
- [16] M. Gadina, M. Lei, D. Schwartz, O. Silvennoinen, S. Nkayamada, K. Yamaoka, J. John, Janus kinase to jakinibs: from basic insights to clinical practice, *Rheumatology* 58 (2019) i14-i16, <https://doi.org/10.1093/rheumatology/key432>.
- [17] G. Thoma, P. Druckes, H. Zerwes, Selective inhibitors of the Janus Kinase JAK3 - Are they effective? *Bioorg. Med. Chem. Lett.* 24 (2014) 4617-4621, <https://doi.org/10.1016/j.bmcl.2014.08.046>.
- [18] M. Clark, K. George, R. Bookland, J. Chen, S. Laughlin, K. Thakur, W. Lee, J. Davis, E. Cabrera, T. Brugel, J. VanRens, M. Laufferweiler, J. Maier, M. Sabat, A. Golebiowski, V. Easwaran, M. Webster, B. Dea, G. Zhanga, Development of new pyromopyrimidine-based inhibitors of Janus kinase 3 (JAK3), *Bioorg. Med. Chem. Lett.* 17 (2007) 1250-1253, <https://doi.org/10.1016/j.bmcl.2006.12.018>.
- [19] Y. Nakajima, T. Inoue, K. Nakai, K. Mukoyoshi, H. Hamaguchi, K. Hatanaka, H. Sasaki, A. Tanaka, F. Takahashi, S. Kunikawa, H. Usuda, A. Moritomo, Y. Higashi, M. Inami, S. Shirakami, Synthesis and evaluation of novel 1H-pyrrolo [2,3-b] pyrimidine -5- carboxamide derivatives as potent and orally efficacious immunomodulators targeting JAK 3, *Bioorg. Med. Chem.* 23 (2015) 4871-4883, <https://doi.org/10.1016/j.bmc.2015.05.034>.
- [20] H. Yamagishi, S. Shirakami, Y. Nakajima, A. Tanaka, F. Takahashi, H. Hamaguchi, K. Hatanaka, A. Moritomo, M. Inami, Y. Higashi, T. Inoue, Discovery of 3,6-dihydroimidazo[4,5-d] pyrrolo [2,3-b] pyridine - 2 (1H) - one derivatives as novel JAK inhibitors, *Bioorg. Med. Chem.* 23 (2015) 4846-4859, <https://doi.org/10.1016/j.bmc.2015.05.028>.
- [21] K. Kaur, S. Kalra, S. Kaushak, Systematic review of tofacitinib: a new drug for the management of rheumatoid arthritis, *Clin. Ther.* 36 (2014) 1074-1086, <https://doi.org/10.1016/j.clinthera.2014.06.018>.
- [22] G. Sanchez, A. Reinhardt, S. Ramsey, H. Wittkowski, P. Hashkes, Y. Berkun, S. Schalm, S. Murias, J. Dare, D. Brown, D. Stone, L. Gao, T. Klausmeier, D. Foell, A. Jesus, D. Chapelle, H. Kim, S. Dill, R. Colbert, L. Failla, B. Kost, M. O'Brien, J. Reynolds, L. Folio, K. Calvo, S. Paul, N. Weir, A. Brofferio, A. Soldatos, A. Biancotto, E. Cowen, J. Digiiovanna, M. Gadina, A. Lipton, C. Hadigan, S. Holland, J. Fontana, A. Alawad, R. Brown, K. Rother, T. Heller, K. Brooks, P. Kumar, S. Brooks, M. Waldman, H. Singh, V. Nickeleit, M. Silk, A. Prakash, J. Janes, S. Ozen, P. Wakim, P. Brogan, W. Macias, R. Goldbach-Mansky, Jak1/2 inhibition with baricitinib in the treatment of autoinflammatory interferonopathies, *J. Clin. Investig.* 28 (2018) 3041-3052, <https://doi.org/10.1172/JCI98814>.
- [23] C. Harrison, A. Vannucchi, U. Platzbecker, F. Cervantes, V. Gupta, D. Lavie, F. Passamonti, E. Winton, H. Dong, J. Kawashima, J. Maltzman, J. Kiladjian, S. Verstovsek, Momelotinib versus best available therapy in patients with myelofibrosis previously treated with ruxolitinib (SIMPLIFY 2): a randomised, open-label, phase 3 trial, *Lancet Haematol.* 5 (2018) e73-e78, [https://doi.org/10.1016/S2352-3026\(17\)30237-5](https://doi.org/10.1016/S2352-3026(17)30237-5).
- [24] C. Harrison, N. Schaap, A. Vannucchi, J. Kiladjian, R. Tiu, P. Zachee, E. Jourdan, E. Winton, R. Silver, H. Schouten, F. Passamonti, S. Zweegman, M. Talpaz, J. Lager, S. Shun, R. Mesa, Janus kinase-2 inhibitor fedratinib in patients with myelofibrosis previously treated with ruxolitinib (JAKARTA-2): a single-arm, open-label, non-randomised, phase 2, multicentre study, *Lancet Haematol.* 4 (2017) e317-e324, [https://doi.org/10.1016/S2352-3026\(17\)30088-1](https://doi.org/10.1016/S2352-3026(17)30088-1).
- [25] M. Blunt, S. Koehrer, R. Dobson, M. Larrayoz, S. Wilmore, A. Hayman, J. Parnell, L. Smith, A. Davies, P. Johnson, P. Conley, A. Pandey, J. Strefford, F. Stevenson, G. Packham, F. Forconi, G. Coffey, J. Burger, A. Steele, The dual syk/JAK inhibitor cerdulatinib antagonises B-cell receptor and microenvironment signaling in chronic lymphocytic leukemia, *Clin. Cancer Res.* 23 (2017) 2313-2324, <https://doi.org/10.1158/1078-0432.CCR-16-1662>.
- [26] S. Lynch, J. DeVicente, J. Hermann, S. Jaime-Figueroa, S. Jin, A. Kuglstatler, H. Li, A. Lovey, J. Menke, L. Niu, V. Patel, D. Roy, M. Soth, S. Steiner, P. Tivimahaision, M. Vu, C. Yee, Strategic use of conformational bias and structure based design to identify potent JAK 3 inhibitors with improved selectivity against the JAK family and kinome, *Bioorg. Med. Chem. Lett.* 23 (2013) 2793-2800, <https://doi.org/10.1016/j.bmcl.2013.02.012>.
- [27] E.R. Goedken, M.A. Argiriadi, D.L. Banach, B.A. Fiamengo, S.E. Foley, K.E. Frank, J.S. George, C.M. Harris, A.D. Hobson, D.C. Ihle, D. Marcotte, P.J. Merta, M.E. Michalak, S.E. Murdock, M.J. Tomlinson, J.W. Voss, Tricyclic covalent inhibitors selectively target JAK3 through an active site thiol, *J. Biol. Chem.* 290 (2015) 4573-4589, <https://doi.org/10.1074/jbc.M114.595181>.
- [28] L. Tan, K. Akahane, R. McNally, K.M.S.E. Reyskens, S.B. Ficarro, S. Liu, G.S. Herter-Sprie, S. Koyama, M.J. Pattison, K. Labela, L. Johannessen, E.A. Akbay, K.-K. Wong, D.A. Frank, J.A. Marto, T.A. Look, J.S.C. Arthur, M.J. Eck, N.S. Gray, Development of selective covalent Janus kinase 3 inhibitors, *J. Med. Chem.* 58 (2015) 6589-6606, <https://doi.org/10.1021/acs.jmedchem.5b00710>.
- [29] A. Thorarensen, M.E. Dowty, M.E. Banker, B. Juba, J. Jussif, T. Lin, F. Vincent, R.M. Czerwinski, A. Casimiro-Garcia, R. Unwalla, J.I. Trujillo, S. Liang, P. Balbo, Y. Che, A.M. Gilbert, M.F. Brown, M. Hayward, J. Montgomery, L. Leung, X. Yang, S. Soucy, M. Hegen, J. Coe, J. Langille, F. Vajdos, J. Chrenok, J.-B. Telliez, Design of a Janus Kinase 3 (JAK3) Specific inhibitor 1-((2S,5R)-5-((7H-pyrrolo[2,3-D]pyrimidin-4-yl)amino)-2-methylpiperidin-1-yl)- prop-2-en-1-one (PF-06651600) allowing for the interrogation of JAK3 signaling in humans, *J. Med. Chem.* 60 (2017) 1971-1993, <https://doi.org/10.1021/acs.jmedchem.6b01694>.
- [30] N. London, R.M. Miller, S. Krishnan, K. Uchida, J.J. Irwin, O. Eidam, L. Gibold, P. Cimernancic, R. Bonnet, B.K. Shoichet, et al., (2014) Covalent docking of large libraries for the discovery of chemical probes, *Nat. Chem. Biol.* 10 (2014) 1066-1072, <https://doi.org/10.1038/nchembio.1666>.
- [31] T. Pravin, A. Anil, J. Mukul, G. Sanjay, Heterocyclic Compounds, WO 2013/054351 A1.
- [32] J. Malerich, J. Lam, B. Hart, R. Fine, B. Klebansky, M. Tanga, A. D'Andrea, Diamino-1,2,4-triazole derivatives are selective inhibitors of TYK2 and JAK1 over JAK2 and JAK3, *Bioorg. Med. Chem. Lett.* 20 (2010) 7454-7457, <https://doi.org/10.1016/j.bmcl.2010.10.026>.
- [33] T. Lin, M. Hegen, E. Quadros, C. Nickerson-Nutter, K. Appell, A. Cole, Y. Shao, S. Tam, M. Ohlmeyer, B. Wang, D. Goodwin, E. Kimble, J. Quintero, M. Gao, P. Symanowicz, C. Wrocklage, J. Lussier, S. Schelling, A. Hewet, D. Xuan, R. Krykbaev, J. Toghias, X. Xu, R. Harrison, T. Mansour, M. Collins, J. Clark, M. Webb, K. Seidl, Selective functional inhibition of JAK-3 is sufficient for efficacy in collagen-induced arthritis in mice, *Arthritis Rheum.* 62 (2010) 2283-2293, <https://doi.org/10.1002/art.27536>.
- [34] A. Botta, E. Sirignano, A. Popolo, C. Saturnino, S. Terracciano, A. Foglia, M. Sinicropi, P. Longo, S. Di Micco, Identification of lead compounds as inhibitors of STAT3: design, synthesis and bioactivity, *Mol. Inform.* 34 (2015) 689-697, <https://doi.org/10.1002/minf.201500043>.
- [35] Y. Zhao, Y. Liu, D. Zhou, Q. Dai, S. Liu, Anti-arthritis effect of chebulanin on collagen-induced arthritis in mice, *PLoS ONE* (2015) 1-14, <https://doi.org/10.1371/journal.pone.0139052>.
- [36] L. Bevaart, M. Vervoordeldonk, P. Tak, Evaluation of therapeutic targets in animal models of arthritis: How does it relate to rheumatoid arthritis? *Arthritis Rheum.* 62 (2010) 2192-2205, <https://doi.org/10.1002/art.27503>.
- [37] Schrödinger Release, 2018-3: Glide, Schrödinger, LLC, New York, NY, 2018.